Journal of Medicinal Chemistry

Article

Synthesis and Evaluation of Analogues of N-Phthaloyl-L-tryptophan (RG108) as Inhibitors of DNA Methyltransferase 1

Saâdia Asgatay, Christine Champion, Gaël Marloie, Thierry Drujon, Catherine Senamaud-Beaufort, Alexandre Ceccaldi, Alexandre Erdmann, Arumugam Rajavelu, Philippe Schambel, Albert Jeltsch, Olivier LEQUIN, Philippe Karoyan, Paola Barbara Arimondo, and Dominique Guianvarc'h

J. Med. Chem., **Just Accepted Manuscript** • Publication Date (Web): 13 Dec 2013

Journal of Medicinal Chemistry is published by the American Chemical Society. 1155 Sixteenth Street N.W., Washington, DC 20036

Synthesis and Evaluation of Analogues of *N*-Phthaloyl-L-tryptophan (RG108) as Inhibitors of DNA Methyltransferase 1

Saâdia Asgatay,# Christine Champion,$† Gaël Marloie,# Thierry Drujon,# Catherine Senamaud-Beaufort,$ Alexandre Ceccaldi,$† Alexandre Erdmann,‡ Arumugam Rajavelu,£ Philippe Schambel,∫ Albert Jeltsch,£ Olivier Lequin,# Philippe Karoyan,# Paola B. Arimondo, $‡, Dominique Guianvarc'h#**

#Laboratoire des BioMolécules, UMR 7203, Université Pierre et Marie Curie-Paris 6 - ENS - CNRS, 4, place Jussieu, 75252 Paris Cedex 05, France. $MNHN CNRS UMR 7196, INSERM U565, 43 rue Cuvier 75005 Paris France. †UPMC Université Paris 6, 75005 Paris, France. £ Institute of Biochemistry, Faculty of Chemistry, University Stuttgart, Pfaffenwaldring 55, 70569 Stuttgart, Germany. ∫Institut de Recherche Pierre Fabre, Centre de Recherche Pierre Fabre, 17 rue Jean Moulin, 81 106 Castres cedex, France. ‡USR ETaC CNRS-Pierre Fabre n°3388 – CRDPF BP 13562, 3 avenue Hubert Curien 31 100 Toulouse France

KEYWORDS. DNA methyltransferase, inhibitors, conformationally constrained analogs, RG108, epigenetics.

ABSTRACT.

DNA methyltransferases (DNMT) are promising drug targets in cancer provided that new, more specific, and chemically stable inhibitors are discovered. Among the non-nucleoside DNMT inhibitors, *N*-Phthaloyl-L-tryptophan **1** (RG108) was first identified as inhibitor of DNMT1. Here, **1** analogs were synthesized to understand its interaction with DNMT. The indole, carboxylate and phthalimide moieties were modified. Homologated and conformationally constrained analogs were prepared. The latter were synthesized from prolino-homotryptophan derivatives through a methodology based amino-zinc-ene-enolate cyclization. All compounds were tested for their ability to inhibit DNMT1 *in vitro*. Among them, constrained compounds **16-18** and NPys derivatives **10-11** were found at least 10-fold more potent than the reference compound. The cytotoxicity on the tumor DU145 cell line of the most potent inhibitors was correlated to their inhibitory potency. Finally, docking studies were conducted in order to understand their binding mode. This study provides insights for the design of the next-generation of DNMT inhibitors.

INTRODUCTION

DNA methylation is an epigenetically inherited chemical modification that is implicated in gene expression regulation.[1] In humans, DNA methylation occurs at position 5 of the cytidine mainly in a CpG context. CpG sequences are not distributed randomly in the genome but are grouped in CpG islands overrepresented in gene promoter regions, in transposons and repeated elements.[2,3]

Methylation of CpG-rich promoters is often associated with transcription inhibition and methylation of repeated regions ensures the stability of the genome. Epigenetic regulation plays an important role not only in the normal functioning of cells (as in embryonic development, cellular differentiation, imprinting, chromosome X inactivation), but also in pathologies and particularly in cancers.[4,5,6,7] Indeed, in tumorigenesis, the epigenetic regulatory system is disrupted leading to global hypomethylation and inappropriate hypermethylation of CpG islands, and thus to aberrant expression of a battery of genes involved in critical cellular processes, from DNA damage repair to apoptosis, cell cycle control, hormone response, cell adhesion/metastasis, and carcinogen detoxification. The first example of CpG methylation of a tumor suppressor gene in a human cancer was described for *Rb* (retinoblastoma) in 1989,[8] but it is not until very recently that this process has been confirmed for other genes and its importance as drug target has been understood.[9] Interestingly, DNA methylation is reversible, thus potentially allowing malignant cells to revert to a more normal state leading to their proliferation arrest and ultimately to their death.[10] The methylation process is carried out by the C5-DNA methyltransferases (DNMTs)[11] and it has been shown that upon use of DNMT inhibitors it is possible to reactivate genes silenced by promoter methylation in cancers.[12,13,14] So, DNMTs are valuable candidate targets for anticancer therapy and several efforts are directed toward developing small molecules that target these enzymes. Most active compounds are nucleosides analogs such as 5-aza-cytidine (5-aza-C) and 5-aza-deoxycytidine (5-aza-dC), which, once incorporated in DNA in place of cytosine, covalently block the DNMT on position 6 of the nucleotide (Figure 1). 5-aza-C and 5-aza-dC have been both approved by FDA for myelodysplastic syndromes and acute myeloid leukemia, and are currently used in clinical trials (Phases II, III) for other cancers.[15,16] Zebularine is also a nucleoside analog that stabilizes the DNMT-DNA complex and shows a lower

cytotoxicity. However, in comparison to the irreversible analogues, zebularine has to be used at higher concentrations to obtain the same demethylation effect in cells, and thus never entered clinical trials. The azanucleosides are very efficient but exhibit little selectivity due to their incorporation everywhere in the DNA and are chemically unstable although some efforts have been made in this area, as evidenced by the identification of the dinucleotide 5-aza-dC followed by a deoxyguanosine (SGI-110) (Figure 1) that shows a better pharmacokinetic profile.[17] This compound is also in clinical trials for the treatment of myelodysplastic syndromes, acute myeloid leukemia and solid tumors. Non-nucleoside analogs have also been found to inhibit DNA methylation, even if their mechanism of action has not been systematically elucidated yet.[18] This inhibitors' family is extremely heterogeneous due to the various chemical structures of the compounds but also to their inhibitory mechanisms, which are not always clearly identified. It includes natural compounds like tea polyphenol[19], (-)-epigallocatechin-3-gallate (EGCG)[20], genistein[21], nanaomycin A[22], psammaplin A[23] or most recently laccaic acid A,[24] and also synthetic drugs already used in the treatment of other pathologies like hypertension (hydralazine[25]), or as local anesthetic (procainamide and procaine[26,27]) (Figure 1). Over the past few years, various DNMT inhibitor compounds were discovered from virtual screenings by the Lyko's group[28,29], among which *N*-Phthaloyl-L-tryptophan **1** that will be further discussed (Figure 1).[30,31] More recently, a quinoline derivative (SGI-1027), which was initially synthesized for its antitumor activities, was reported as an efficient DNMT inhibitor both *in vitro* and in cells (Figure 1).[32] *S*-adenosyl-L-homocysteine (AdoHcy) analogs were also described as inhibitors of human DNMTs but these compounds suffer from low specificity toward DNMTs, because they target other *S*-adenosyl-L-methionine (AdoMet)-dependent methyltransferases as well.[33,34] In summary, today there are several DNMT inhibitors known, but the high toxicity, lack of

specificity, weak activity or chemical instability of these molecules hinder their use.[35] Therefore, there is a great need to design new drugs that specifically target DNMTs. Currently, the non-nucleoside-based analogs are more interesting to develop and, in an effort to discover new compounds, we recently developed several strategies. First, we have set up a HTS based on fluorescence detection to find new inhibitors of DNMT from chemical libraries, allowing the characterization of promising flavones and flavanones derivatives (Figure 1) with IC_{50} in the nanomolar range.[36] In a second approach, we increased the inhibitors activity by conjugating them to a DNA ligand. We chose procainamide as a DNA binder to guide an inhibitor of DNMT to CpG-rich regions, in order to increase its local concentration at CpG sites (Figure 1).[37] The pharmacomodulation of non-nucleosidic validated inhibitors specific for DNMTs constitutes a third strategy to increase the potency of these inhibitors. Among them, **1**, a non-nucleoside inhibitor discovered from an *in silico* screen,[30,31] presents some interesting features (Figure 1). Indeed, it has been shown to inhibit DNMT in a non-covalent manner and to cause demethylation of genomic DNA in cells without any detectable toxicity.[30] More recently, maleimide derivatives of **1** were designed to trap DNMT1 through addition of the catalytic thiol of the enzyme to the maleimide moiety (Figure 1).[38] Herein, we conducted a structure-activity relationship (SAR) study to understand the important features of **1** and its interaction in the DNMT active site, in order to improve its activity. We synthesized a small library of analogs of **1** shown in Figure 2. We chose to modify the indole, carboxylate and phthalimide moieties. We designed also constrained analogs to partially reduce the flexibility of the inhibitor. This strategy was recently used to improve other DNMT inhibitors such as: procaine and AdoHCy (Figure 1).[39,40] Finally, we also synthesized β2- and β3-phthaloylated homotryptophane as homologated

compounds. We report here the synthesis, the biological activity and a structural study of these derivatives of **1**.

Chemistry

Synthesis of compounds 2-11 (Figure 2). The compounds **1**(*S*), **1**(*R*), **2-6** and **8** were obtained from the commercially available corresponding amino acids L-tryptophan, D-tryptophan, 5-hydroxy-L-tryptophan, L-histidine, L-phenylalanine, 3-benzothienyl-L-alanine, 3-(2-oxo-1,2-dihydro-4-quinolinyl)-L-alanine and L-tryptophanamide, respectively, according to Casimir *et al.*'s procedure (Scheme 1).[41] The methyl 2-((succinimidooxy)carbonyl)benzoate (MSB) was reacted with the sodium salt of the corresponding amino acid in water/acetonitrile affording the corresponding phthaloylated compounds **2-6**, **8** in good yields. The tryptophan quinazolinedione derivative **9** was obtained by reacting 2-carbomethoxyphenyl isocyanate **20** with L-tryptophan (L-Trp) in a mixture of dioxane and water containing NaOH 1M at 50°C following the method reported by Canonne *et al.* (Scheme 2).[42] Synthesis of **10** and **11** were achieved in good yields by treatment of L-tryptophan with 2-nitropyridinylsulfenyl chloride and 2,4-dinitrophenylsulfenyl chloride, respectively, in aqueous alkaline solution (Scheme 2).

Synthesis of homologated analogues 12-14 (Figure 2). β2-phthaloyl-homotryptophan **12**(*R*) and **12**(*S*) were obtained from the corresponding β2-homotryptophan **26** by using the same phthaloylation procedure as described in Scheme 1. For the synthesis of β2-homotryptophan, we used the diastereoselective methodology based on aminomethylation of chiral silyl enol ether recently described by Moumné *et al.* (Scheme 3).[43] This method allows the preparation of enantiomerically pure functionalized β2-amino acids. Briefly, 3-indolylpropanoic acid **21** was *N*-benzylated leading to compound **22** that was activated to the corresponding mixed anhydride

with isobutyl chloroformate and coupled to (+) or (-) Oppolzer's Sultam as chiral-auxiliary (in accordance with the desired enantiomer) to give **23** in 55% overall yield. In the key step of the synthesis, **23** was converted to the silyl enol ether intermediate that was aminomethylated in the presence of highly reactive trifluoroacetate dibenzylidene imminium salt to give **24** in 88% yield. Finally, β2-homotryptophan **26** was obtained after successive protection/deprotection steps, *i.e.* (*i*) deprotection of the dibenzylamine moiety by hydrogenolysis, (*ii*) removal of the Sultam moiety by saponification, (*iii*) Boc amine protection, (*iv*) deprotection of the indole under Birch conditions and (*v*) amine deprotection in TFA.

β3-phthaloyl-homotryptophan **13** was obtained from the commercially available corresponding β3-homotryptophan upon use of the same phthaloylation procedure as described in Scheme 1. The dipeptide **14** was obtained by coupling L-tryptophan benzyl ester and the phthaloyl glycine **7** that was activated to the corresponding mixed anhydride with isobutyl chloroformate in THF at -15°C affording the dipeptide **27**. Next, **27** was debenzylated by catalytic hydrogenation over palladium charcoal to afford **14** in good yield (Scheme 4).

Synthesis of constrained analogues 15-18 (Figure 2). The constrained analogues **15-18** were obtained from the Boc protected prolino-homotryptophan derivative **30** (Scheme 5). This compound was synthesized through a methodology developed by Mothes *et al.* based on amino-zinc-ene-enolate cyclization.[44] Carbocyclization of olefin **28** was achieved after deprotonation with LDA and transmetallation in the presence of $ZnBr_2$. Compound **29** was obtained through Negishi cross-coupling of the *N*-Boc-3-iodo-indole with the cyclic zinc intermediate by using $Pd(OAc)_2$ in the presence of (*t*-Bu_3PH)-BF_4. **29** was debenzylated by catalytic hydrogenation over palladium charcoal affording **30**. Finally, **15**, **16** and **17** were obtained after reacting **30** in the presence of *N*-phthaloylglycine **7**, naphthoyl or benzoyl chloride, respectively, and

deprotection in TFA. **30** was also treated with 2,4-dinitrophenylsulfenyl chloride and **18** was obtained after deprotection in TFA.

RESULTS AND DISCUSSION

1 is a rationally designed small molecule inhibitor of DNMT that was found by computational screening of a database of compounds with potential high affinity to a three-dimensional model of the human DNMT1 catalytic pocket.[45] Since at that time the X-ray structure of DNMT1 was not available, this model was established by using a homology modeling approach with known structures of bacterial C5-DNMT (M. Hha I and M. Hae III) and human DNMT2.[46]

Actually, the precise molecular mode of action of this inhibitor is not known but it presumably acts by blocking the active site of the enzyme, as predicted by the molecular modeling study. According to Siedlecki *et al.*[45,46], the phthalimide moiety seems to occupy the same part of the binding pocket as the native cytosine. In addition, the docking study suggested that (*i*) the anionic carboxylate group of **1** plays a critical role and makes hydrogen bonds with Arg 1310, and (*ii*) the phthalimide group lies next to the catalytic cysteine in the active site of DNMT1, making a hydrogen bond through its carbonyl to Arg 1308.[45] By saturation transfer difference (STD) NMR spectroscopy experiments, we observed that **1** interacts with human DNMT1, the catalytic domain of murine Dnmt3A and the catalytic complex of murine Dnmt3A/3L.[37] Suzuki et al.[38] docked the maleimide derivatives of **1** in the crystal structure of M.Hha I. They found that the indole ring is located in a hydrophobic pocket formed by Tyr254, Gly88 and Gly255, while the carboxylate forms two hydrogen bonds with Arg163. Thus, the features implicated in the binding interaction with the enzyme are still not fully elucidated. In this context, we have undertaken a systematic *in vitro* study to explore the contributions of each functional group of

the molecule to the binding. All synthesized compounds were tested in an *in vitro* DNA methylation assay, measuring the incorporation of tritiated methyl from ^{3}H-labeled AdoMet by human recombinant DNMT1 into a hemimethylated DNA duplex as substrate. All compounds were first tested at 500 μM in the DNMT1 inhibition activity assay (Figure 3) and next, the inhibitory concentration IC_{50} was evaluated on DNMT1 for our most efficient compounds to further explore their inhibitory efficiency (Table 1).

Since the activity of a racemic mixture of **1** was initially reported,[30,45] we studied whether the configuration of the asymmetric carbon plays an important role in the inhibitory activity and established the stereospecificity of the activity. In our enzyme assay, **1**(*S*) showed only a modest IC_{50} value of 390 μM in comparison with the 115 nM value initially reported by the authors describing **1** activity.[30] In fact, their value was obtained on the bacterial DNMT M.Sss I and using an unmethylated DNA substrate. In addition, the two biological tests are different: here, we measured the direct incorporation of a radiolabeled methyl group on a short hemimethylated DNA substrate containing 8 CpGs and not the indirect inhibition of a restriction enzyme by methylation of a 798 pb DNA substrate containing several CpGs. Actually, notorious variations in compounds activity in DNMT inhibition enzymatic tests have already been observed in other studies[47] and depend on the assay and the chosen DNA substrate. However, our data are in agreement with the recent findings of Suzuki *et al.* reporting a 34% inhibition of recombinant human DNMT1 activity at **1** concentration of 1 mM.[38] **1**(*R*) showed an activity comparable to **1**(*S*) and was shown to bind to DNMT by NMR using STD experiments. This result led us to reassess the interaction model proposed above. In order to further characterize the binding mode of **1**, we investigated whether **1** could compete with known ligands of DNMT by 1D NMR spectroscopy. Indeed, the binding of **1** and AdoHcy ligands was followed using WaterLOGSY

(Water-Ligand Observed via Gradient SpectroscopY).[48,49,50] This experiment relies on the observation of intermolecular NOE magnetization transfer via bulk water. Small molecules in solution are characterized by positive NOEs with bulk water while ligands interacting in fast exchange with macromolecules typically have negative NOEs. This NMR study was carried out on the murine catalytic domain of Dnmt3A, a DNMT model available in large amounts. As shown in Figure 4, the adenine protons of AdoHcy display positive NOEs in the absence of Dnmt3A (Figure 4b) whereas in the presence of Dnmt3A the NOE signals are cancelled or become negative (Figure 4c), indicating that AdoHcy interacts with the enzyme. The addition of **1** (Figure 4d) leads to a 50% reduction in the intensity of the negative NOE and the appearance of a positive NOE for the AdoHcy protons resonating at 8.26 and 8.36 ppm, respectively, indicating decreased binding of AdoHcy. In addition, **1** protons exhibit strong negative NOEs due to the binding to Dnmt3A. These NMR observations indicate that **1** and AdoHcy compete for binding to Dnmt3A, leading to a new interaction model for **1**.

In quest of determinants of **1** binding to DNMT, we chose to modify each functional group of the compound: the indole, the carboxylate and the phthalimide moiety. The derivatives lacking the indole or phthalimide moiety, *i.e.* phthaloyl glycine **7** and L-tryptophan, respectively, were inactive at 500 μM, emphasizing the need for these pharmacophores. Several indole substituents were tested. The replacement of indole by a most acid heterocycle such as imidazole (compound **3**), by a non-heterocyclic phenyl group (compound **4**) or by a quinolone moiety (compound **6**) was unfavorable as these modifications resulted in the absence of inhibitory potency at 500 μM. A 5-hydroxy derivative **2** was also tested, because it was the starting material for the synthesis of conjugated compounds. Indeed, according to the modeling of Lyko's group[45], the 5-position of the tryptophan sticks out of the DNMT active site. Accordingly, a conjugated biotinylated

derivative of **1** was already synthesized.[51] No significant difference was observed between compounds **1** and **2** validating the 5-position of the tryptophan as an anchor point for potential linkers. Interestingly, bioisosteric replacement of the indole moiety by the bicyclic benzothiophene (*i.e.*, variation of the heteroatom from nitrogen to sulfur) was favorable since the analog **5** is 2-fold better than **1** with an IC_{50} of 230 μM. Thus, the replacement of the good H-bond donor NH group by a poor H-bond acceptor sulfur atom led to a better inhibitory efficacy, indicating that the DNMT binding pocket is sensitive to changes in the electronic character of the aromatic system. With regard to the phthalimide group, we replaced it by a quinazolinedione substituent (compound **9**) by assuming that it could mimic the pyrimidine ring of cytidine as the phthalimide moiety was supposed to occupy the same part of the binding pocket as cytosine.[45,46] However, this modification did not dramatically affect the activity. Most interestingly, the phthalimide moiety was favorably replaced by Npys group or 2,4-dinitrobenzenesulfenyl: compounds **10** and **11** showed an important increase in activity with IC_{50} values of 20 and 40 μM, respectively, a 20- and 10-fold gain in comparison with **1**. We already observed the importance of the presence of an electron withdrawing group such as nitro through our previous study on another DNMT inhibitors family, *i.e.* flavanones.[36] To determine the contribution of the negative charge of the carboxylate group in **1**/DNMT interaction, we replaced the carboxylate group by a neutral isosteric amide function in tryptophanamide **8**. Indeed, an analogue of **1**, named RG119 that lacks the carboxylate group was previously reported as inactive in demethylating genomic DNA.[30] **8** showed a low activity at 500 μM similar to that of **1**, so the determinant role of the negative charge in **1** activity seems to be inconclusive.

Next, we examined whether an extension of compound **1** could better occupy the space of the binding pocket and possibly improve the binding affinity for DNMT1. For this purpose,

homologated analogs of **1** were synthesized in order to explore the space of the ligand binding site. Two isomers of phthaloylated β-tryptophan, which have their amino group bound to carbon β instead of α, were assayed: β2, in which the side chain is also bound to carbon β (compounds **12**(*R*) and **12**(*S*)), and β3-tryptophan, in which the side chain is bound to carbon α (compound **13**). Furthermore, a dipeptide *N*-Pht-GlyTrp **14** was assayed. Unfortunately, no significant improvement in activity was observed with this family of compounds. This could be explained by the fact that the important moieties of the compound are located too far away to each other.

Finally, we attempted to restrict **1** to a bioactive conformer by reducing its flexibility. The two enantiomers of a prolino analogue of tryptophan were synthesized and different aromatic substituents were conjugated to the amine moiety of the proline ring in order to mimic the phthaloyl part. When phthaloylglycine was conjugated through a peptide link in order to mimic the phthaloyl moiety of **1** (see compound **15**), no improvement in activity was observed in comparison with **1**. Interestingly, the linkage of a benzoyl or naphthoyl moiety was favorable and compounds **16** and **17** showed increased activity with 50 to 100% inhibition at 500 μM. IC_{50} determinations for these compounds confirmed their potent inhibition activity: IC_{50} values ranging from 128 to 50 μM were obtained as compared to 390 μM for reference compound **1**. Noteworthy, in each series of prolino derivatives, the enantiomer (2*R*,3*S*) was always the most active. The compound bearing the naphthoyl moiety (**16**) showed a slightly better activity than the compound with the benzoyl one (**17**) (IC_{50} of 50 μM and 73 μM respectively, for the most active enantiomer **16** and **17**). Therefore, the prolino compounds constitute a promising new family of **1** derivatives since our better constrained analog **16** (2*R*,3*S*) is 8-fold better than **1**. The important features of each best compound found in this study were associated in compound **18** (2*R*,3*S*): a prolino analog of tryptophan bearing a Npys substituent. Unfortunately, we did not

obtain the expected synergic activity since an IC_{50} value of 80 μM was obtained, which is comparable to that of compound **17** (2*R*,3*S*).

Finally, we determined the cytotoxicity of the most potent inhibitors on prostate cancer cells DU145 (Table 1). We chose this cell line for our study as methylation-mediated repression of suppressor tumor genes was clearly observed in prostate cancer[4] and their reactivation constitutes a potential approach for the treatment of this cancer. In the presence of **1**, we observed a modest 660 μM cytotoxicity value. Under the same conditions, the prolino compounds, the 2-nitropyridinylsulfenyl and 2,4-dinitrobenzenesulfenyl derivatives showed lower TC_{50} values (2 to 6 fold). Interestingly, a link between IC_{50} and TC_{50} was observed for the enantiomers of compound **16**: the **16** (2*R*, 3*S*) enantiomer is the most active on DNMT1 as well as in terms of cytotoxicity. This correlation is less clear in the case of compound **17**, as the difference in inhibition activity is smaller. However, in general the best DNMT inhibitors showed the highest cytotoxicities. In conclusion, the cytotoxicity values obtained with the compounds are improved in comparison to that observed with **1**, but these values remain modest, the best compound showing a 100 μM cytotoxicity.

In order to understand the gain in activity for the most potent compounds, molecular docking studies were carried out on a three-dimensional model of murine catalytic Dnmt1 (residues 732-1600) built from the X-ray structure of the catalytic complex (PDB 4DA4).[52] The choice of this structure has been guided by the fact that we wanted to start from a model in which both the cofactor, here the product AdoHcy, and the DNA substrate, cytidine, are well-resolved, together with the BAH1, BAH2 and the entire MTase domain, even though the CXXC domain (residues 646-692) and the autoinhibitory linker domain (residues 699-733) are lacking. Induced-fit docking (IFD) studies were carried out with the constrained analogs **16** and **17**. The IFD

procedure was validated upon docking of the AdoHcy exactly as the ligand of the crystal structure (Supplementary Figure 1). **1** was found in the AdoMet pocket (Figure 5A); its carboxyl group interacts with Lys1247 and Arg 1576 and the carbonyl of the phthalimide interacts also with Lys1247 (Figure 5B). This result is consistent with our NMR study showing that **1** and AdoHcy compete in binding to DNMT. Figure 5C compares **1** and the most potent maleimide derivative of Suzuki et *al.* (compound 5 of their article).[38] Both compounds are perfectly superimposed and the same interactions with Arg1576 and Lys1247 were found. The SYBYL-X 1.3 software revealed a partially different positioning in the MTase catalytic site for **1** and the maleimide derivative compared to previous findings on DNMT1[45] and M. Hha I,[38] respectively. Inhibitors **16** (Figure 5D) and **17** (Supplementary Figure S2) fit the AdoMet pocket and interact through the carboxyl with Lys1247 as **1** (Figure 5E and Supplementary Figure S2). In addition, the proline group fits in the ribose pocket of the cofactor and, unexpectedly, the naphthoyl and the benzoyl fit towards the cytidine pocket of the crystal structure, forming an interaction with Arg1576 through the carbonyl of the substituent. These compounds thus fill the entire accessible catalytic pocket, thereby explaining their higher inhibition activity (up to 8-fold). Similarly, the IFD analysis suggested that compound **11**, 10-fold more potent than **1**, also occupies the same pockets (data not shown). Concerning compound **5**, its superior inhibitory efficacy could be explained by the hydrophobic nature of the pocket, in which the indole moiety binds.

The main conclusion regarding the interaction of the constrained analogues with both the DNA and AdoMet pockets was further confirmed by a selectivity assay performed on compound **17** (2*R*, 3*S*). Indeed, we investigated whether **17** could affect the activity of other methyltransferases in order to get insights on the mechanism of inhibition. **17** was tested against the histone methyltransferase (HMTK) G9a, which methylates histone tails on their lysine residues,[53] and

the bacterial DNA (adenine *N*-6)-methyltransferase, EcoDam, which methylates DNA at the adenine within GATC sites.[54,55,56] A biotin–avidin microplate kinetic assay based on ^{3}H-SAM incorporation was used for the quantitative analysis of methyltransferase activities *in vitro*.[57] Interestingly, **17** showed a very good specificity for the DNMT1, as compared to the other two methyltransferases, since it did not affect the other methyltransferase activities (up to a concentration of 750 μM for EcoDam and 1 mM for G9a), while the IC_{50} for DNMT1 was 73 μM (Table 1).

CONCLUSION

The non-nucleosidic DNMT inhibitors constitute a heterogeneous family of compounds with a high potential therapeutic interest but more data are needed to understand their mode of action. In this context, we examined *N*-Phthaloyl-L-tryptophan **1**, because it was described as the first specific inhibitor of DNMT. Our systematic study showed that both the indole and phthaloyl moieties are required to observe an inhibitory effect. However, it is possible to improve **1** by replacing these groups by a benzothiophene and Npys group or 2,4-dinitrobenzenesulfenyl, respectively. Furthermore, constrained analogs also showed an increased efficiency in DNMT1 inhibition. A molecular modeling study led us to propose the following hypothesis explaining the higher inhibition activity of the prolino compounds: unlike **1**, which fits in the AdoMet pocket in our model, the prolino compounds fit both the AdoMet and the cytidine pockets, therefore filling the entire accessible catalytic pocket. In conclusion, our study provides a structure-activity-relationship framework to be integrated for the conception of the next generation of DNMT inhibitors. Prolino compounds seem most promising and it would be useful to design derivatives

exhibiting the main features from this study: prolino analogs containing the benzothiophene heterocycle may be envisaged. Moreover, the introduction of substituted naphthoyl moieties, for example with nitro group, should be considered.

EXPERIMENTAL SECTION

Chemistry. Solvents and most of the starting materials were purchased from Sigma Aldrich. **1**(*S*) and **1**(*R*) were prepared according to [41] from L- and D-tryptophan. ^{1}H and ^{13}C NMR spectra were recorded on Bruker ARX 250 and 400 spectrometers. Chemical shifts are given in parts per million (ppm) using the $CDCl_3$ signal as reference ($\delta^{1}H$ = 7.26 ppm, $\delta^{13}C$ = 77.16 ppm) and coupling constants (*J*) are given in Hertz (Hz). All yields reported are unoptimized. Flash chromatography was performed using silica gel Merck 60 with 0.040–0.063 µm. Some compounds were separated and purified by preparative reverse phase HPLC using a Symmetry, C8 (250 x 10 mm; 5µm) column with a multiple gradient of acetonitrile in water at a flow rate of 3 mL/min with UV detection at 220 and 280 nm. Analytical HPLC conditions were as follows: column Waters X Terra MS C18 (250 x 4.6 mm, 5 mm) with a gradient of acetonitrile in water (0 to 100% during 30 min) at a flow rate of 1 mL/min, detection at 220 and 280 nm. Purity of tested compounds was established by analytical reverse phase HPLC confirming a purity of at least 95%. High resolution mass spectra (HRMS) were recorded at the Institut de Chimie Moléculaire (FR 2769) of UPMC (electrospray source).

General Synthetic Method for compounds 2-6, 8, 13.

To a stirred solution of the appropriate amino acid (1 equiv) and sodium carbonate (5 equiv) dissolved in water/acetonitrile, was added methyl 2-((succinimidooxyl)carbonyl)benzoate (2

equiv) freshly prepared.[41] The mixture was vigorously stirred overnight at room temperature. The solution was acidified to pH = 1-2 with 2N HCl, diluted with EtOAc and washed with 1N HCl and water. The organic phase was dried with Na_2SO_4, filtered, and concentrated in vacuo. The product is isolated by preparative reverse phase HPLC, on a Symmetry, C8 (250 x 10 mm; 5µm) column with a multiple gradient of acetonitrile in water (20 to 40% during 5 min, 40 to 45 % during 20 min) at a flow rate of 3 mL/min.

2(*S*)-(1,3-Dihydro-1,3-dioxo-2*H*-isoindol-2-yl)-3-(5-hydroxy-1*H*-indole-3-yl)-propanoic acid (2): light yellow solid, 11 % yield; HPLC Rt = 10.3 min; ^{1}H-NMR (MeOD): δ (ppm) 7.75 (m, 4H); 7.07 (dd, *J* = 0.4 Hz, *J* = 8.5 Hz, 1H); 6.90 (dd, *J* = 0.4 Hz, *J* = 2.2 Hz, 1H); 6.88 (s, 1H); 6.60 (dd, *J* = 2.2 Hz, *J* = 8.7 Hz, 1H); 5.20 (dd, *J* = 11.6 Hz, *J* = 4.8 Hz, 1H); 3.70 (dd, *J* = 15.1 Hz, *J* = 11.4 Hz, 1H); 3.60 (dd, *J* = 14.9 Hz, *J* = 4.8 Hz, 1H). ^{13}C-NMR (MeOD): δ (ppm) 172.59; 169.11; 151.16; 135.43; 132.90; 132.85; 129.13; 124.90; 124.17; 112.65; 112.44; 110.50; 103.22; 54.17; 25.60. HRMS calcd for $C_{19}H_{15}N_2O_5$ [MH^+]: 351.0975. Found: 351.0996

2(*S*)-(1,3-Dihydro-1,3-dioxo-2*H*-isoindol-2-yl)-3-(3*H*-imidazol-4-yl)-propanoic acid (3): white solid, 11 % yield; HPLC Rt = 6.7 min; ^{1}H-NMR (DMSO-d_6): δ (ppm) 8.92 (s, 1H); 7.90 (br s, 4H); 7.44 (s, 1H); 5.11 (dd, *J* = 10.5 Hz, *J* = 4.4 Hz, 1H); 3.54 (dd, *J* = 15.8 Hz, *J* = 4.3 Hz, 1H); 3.38 (dd, *J* = 15.5 Hz, *J* = 10.5 Hz, 1H).^{13}C-NMR (DMSO-d_6): δ (ppm) 169.10; 167.02; 134.97; 134.09; 130.93; 129.31; 123.51; 117.16; 50.99; 24.16. HRMS calcd for $C_{14}H_{12}N_3O_4$ [MH^+]: 286.0822. Found: 286.0802

2(*S*)-(1,3-Dihydro-1,3-dioxo-2*H*-isoindol-2-yl)-3-phenylpropanoic acid (4): white solid, 32 % yield; HPLC Rt = 17 min; ^{1}H-NMR ($CDCl_3$): δ (ppm) 7.77 (m, 2H); 7.67 (m, 2H); 7.17 (m, 5H); 5.19 (dd, *J* = 9.0 Hz, *J* = 6.6 Hz, 1H); 3.55 (m, 2H). ^{13}C-NMR ($CDCl_3$): δ (ppm) 173.56; 167.36;

136.41; 134.14; 131.49; 128.80; 128.60; 126.93; 123.53; 52.99; 34.41. HRMS calcd for $C_{17}H_{14}NNaO_4$ [MNa^+]: 318.0737. Found: 318.0736

3-(Benzothien-3-ylmethyl)-2(*S*)-(1,3-dihydro-1,3-dioxo-2*H*-isoindol-2-yl)-propanoic acid (5): white solid, 30 % yield; HPLC Rt = 22.1 min; ^{1}H-NMR (MeOD): δ (ppm) 7.82 (m, 2H); 7.76 (br s, 4H); 7.31 (m, 2H); 7.23 (s, 1H); 5.31 (dd, *J* = 10.9 Hz, *J* = 5.0 Hz, 1H); 3.86 (dd, *J* = 14.9 Hz, *J* = 10.9 Hz, 1H); 3.79 (dd, *J* = 5.0 Hz, *J* = 15.1 Hz, 1H). ^{13}C-NMR (MeOD): δ 171.97; 168.93; 141.71; 139.77; 135.61; 133.00; 132.78; 125.36; 125.11; 124.85; 124.28; 123.78; 122.32; 99.13; 53.05; 28.56. HRMS calcd for $C_{19}H_{14}NO_4S$ [MH^+]: 352.0638. Found: 352.0628

2(*S*)-(1,3-Dihydro-1,3-dioxo-2*H*-isoindol-2-yl)-4-quinolinepropanoic acid (6): white solid, 19 % yield; HPLC Rt = 17.9 min; ^{1}H-NMR (DMSO-*d6*): δ (ppm) 7.86 (br s, 4H); 7.81 (d, *J* = 8.1 Hz, 1H); 7.48 (dd, *J* = 8.1 Hz, *J* = 7.0 Hz, 1H); 7.28 (d, *J* = 8.3 Hz, 1H); 7.18 (dd, *J* = 8.1 Hz, *J* = 7.0 Hz, 1H); 6.26 (s, 1H); 5.19 (dd, *J* = 10.9 Hz, *J* = 4.4 Hz, 1H); 3.75 (dd, *J* = 14.7 Hz, *J* = 4.4 Hz, 1H); 3.52 (dd, *J* = 14.4 Hz, *J* = 10.9 Hz, 1H). ^{13}C-NMR (DMSO-*d6*): δ (ppm) 169.54; 167.03; 161.03; 147.14; 138.82; 135.01; 130.67; 130.37; 124.00; 123.49; 121.84; 121.65; 118.19; 115.73; 50.91; 30.64. HRMS calcd for $C_{20}H_{15}N_2O_5$ [MH^+]: 363.0975. Found: 363.0972

2(*S*)-(1,3-Dihydro-1,3-dioxo-2*H*-isoindol-2-yl)-3-(1*H*-indole-3-yl)-propanamide (8): light yellow solid, 35 % yield; HPLC Rt = 13 min; ^{1}H-NMR (MeOD): δ (ppm) 7.73 (br s, 4H); 7.55 (d, *J* = 7.9 Hz, 1H); 7.22 (d, *J* = 8.1 Hz, 1H); 7.01 (td, *J* = 1.0 Hz, *J* = 8.12 Hz, *J* = 7.00 Hz, 1H); 6.92 (s, 1H); 6.92 (td, *J* = 1.0 Hz, *J* = 8.0 Hz, *J* = 7.7 Hz, 1H); 5.19 (dd, *J* = 11.4 Hz, *J* = 5.2 Hz, 1H); 3.75 (dd, *J* = 14.7 Hz, *J* = 11.4 Hz, 1H); 3.66 (dd, *J* = 14.7 Hz, *J* = 5.3 Hz, 1H). ^{13}C-NMR (MeOD): δ (ppm) 172.58; 167.88; 136.43; 133.76; 131.62; 126.86; 122.78; 122.54; 120.85; 118.20; 117.62; 110.67; 109.77; 53.99; 24.02. HRMS calcd for $C_{19}H_{16}N_3O_3$ [MH^+]: 334.1186. Found: 334.1221

2(*S*)-(1,3-dihydro-1,3-dioxo-2*H*-isoindol-2-yl)-3-(1*H*-indole-3-yl)- butanoic acid (13): light yellow solid, 26 % yield; HPLC Rt = 15.7 min; ^{1}H-NMR (MeOD): δ (ppm) 10.14 (s, 1H); 7.75 (br s, 4H); 7.58 (d, *J* = 7.9 Hz, 1H); 7.26 (d, *J* = 8.1 Hz, 1H); 6.95 (m, 3H); 4.99 (m, 1H); 3.41 (dd, *J* = 14.2 Hz, *J* = 9.4 Hz, 1H); 3.28 (m, 3H); 2.92 (dd, *J* = 16.0 Hz, *J* = 5.7 Hz, 1H). ^{13}C-NMR (MeOD): δ (ppm) 174.88; 169.75; 137.99; 135.23; 133.03; 128.62; 124.15; 122.33; 119.69; 119.25; 112.18; 111.92; 54.7; 37.5; 29.3. HRMS calcd for $C_{20}H_{16}N_2NaO_4$ [MNa^+]: 371.1002. Found: 371.1003

3(2*H*)-Quinazolineacetic acid, 1,4-dihydro-α-(1*H*-indol-3-ylmethyl)-2,4-dioxo-, (*S*)- (9): The commercially available isocyanate **20** (0.3 mmol) was added to a solution of L-tryptophan (1.5 equiv) in a mixture of 20 mL of water/dioxane (1/1) and sodium hydroxide (1M, 10 mL). The mixture was stirred at 50°C for 4h. The reaction mixture was diluted with H_2O, acidified with hydrochloric acid (10%) to pH = 3 and extracted with EtOAc. The combined organic layers were concentrated in vacuo and the crude residue was purified using reverse phase HPLC, on a Symmetry, C8 (250 x 10 mm; 5µm) column with a multiple gradient of acetonitrile in water (20 to 40% during 5 min, 40 to 45 % during 20 min) at a flow rate of 3mL/min leading to **9** as a white solid, 10 % yield. HPLC Rt = 13.4 min; ^{1}H-NMR (DMSO-*d6*): δ (ppm) 8.30 (d, *J* = 8.5 Hz, 1H); 7.89 (dd, *J* = 1.5 Hz, *J* = 4.6 Hz, 1H); 7.58 (d, *J* = 7.6 Hz, 1H); 7.44 (m, 1H); 7.34 (d, *J* = 7.92 Hz, 1H); 7.18 (d, *J* = 2.4 Hz, 1H); 7.08 (m, 1H); 7.01 (d, *J* = 7.9 Hz, 1H); 6.95 (m, 1H); 4.41 (m, 1H); 3.19 (dd, *J* = 14.2 Hz, *J* = 4.6 Hz, 1H); 3.04 (dd, *J* = 14.4 Hz, *J* = 9.6 Hz, 1H). ^{13}C-NMR (MeOD): δ (ppm) 174.1; 154.5; 142.6; 136.1; 133.5; 127.1; 123.5; 120.9; 120.2; 119.3; 118.3; 118.15; 111.3; 110.2; 53.7; 27.2. HRMS calcd for $C_{19}H_{16}N_3O_4$ [MH^+]: 350.1135. Found: 350.1139

***N*2-[(3-nitro-2-pyridinyl)thio]-L-Tryptophan (10)**: To a solution of L-tryptophan (40 mg) in 2M NaOH (1 mL) and dioxane (5 mL), nitropyridinylsulfenyl chloride (1.1 equiv) was added dropwise over 15 min, whilst 2M NaOH (2 mL) was added dropwise with vigorous stirring. The mixture was diluted with H_2O (50 mL), filtered from precipitated disulfide, overlayered with EtOAc and acidified with 0.5 M H_2SO_4. Upon extraction with EtOAc, the combined extracts were washed twice with H_2O and then dried over Na_2SO_4. The solution was concentrated and purified by HPLC in the same conditions as described above leading to **10** as a yellow solid, 50 % yield. HPLC R_t = 21.6 min; ^{1}H-NMR (MeOD): δ (ppm) 8.50 (dd, *J* = 8.1 Hz, *J* = 1.5 Hz, 1H); 7.98 (dd, *J* = 4.6 Hz, *J* = 1.3 Hz, 1H); 7.59 (d, *J* = 8.1 Hz, 1H); 7.41 (d, *J* = 8.1 Hz, 1H); 7.24 (m, 2H); 7.14 (t, *J* = 7.9 Hz, 1H); 7.02 (t, *J* = 7.9 Hz, 1H); 3.97 (dd, *J* = 8.8 Hz, *J* = 5 Hz, 1H); 3.43 (dd, *J* = 14.5 Hz, *J* = 4.8 Hz, 1H); 3.17 (dd, *J* = 14.5 Hz, *J* = 8.7 Hz, 1H). ^{13}C-NMR (MeOD): δ (ppm) 175.8; 163.8; 154.3; 140.7; 135.0; 129.1; 124.9; 122.4; 120.8; 119.7; 119.5; 118.9; 112.3; 107.0; 65.0; 30.5. HRMS calcd for $C_{16}H_{15}N_4O_4S$ [MH^+]: 359.0808. Found: 359.0797

***N*2-[(2,4-dinitrophenyl)thio]-L-Tryptophan (11)**: **11** was obtained following the same procedure as for compound **10** using 2,4-dinitrophenylsulfenyl chloride instead of nitropyridinylsulfenyl chloride. **11** was obtained as a yellow solid, 70 % yield; HPLC R_t = 24.7 min; ^{1}H-NMR (MeOD): δ (ppm) 8.74 (br s, 1H); 7.55 (m, 1H); 7.43 (m, 2H) ; 7.31 (m, 1H) ; 7.22 (s, 1H); 7.13 (m, 1H); 6.98 (m, 1H); 3.77 (m, 1H); 3.44 (m, 1H); 3.10 (m, 1H). ^{13}C-NMR (MeOD): δ (ppm) 175.8; 160.3; 154.0; 143.9; 141.3; 136.7; 127.3; 125.8; 125.6; 123.8; 121.3; 120.1; 118.9; 118.7; 118.1; 117.6; 111.0; 110.5; 64.7; 28.7. HRMS calcd for $C_{17}H_{15}N_4O_6S$ [MH^+]: 403.0706. Found: 403.0715

(*N*-benzylindoyl) propanoic acid (**22**): To a stirred solution of 3-indolylpropionic acid **21** (10 g) in DMF (55 mL) cooled to 0°C was added sodium hydride (2.2 equiv) slowly. After 30 min,

benzyle bromide (1 equiv) was added. The mixture was allowed to react over 1 h, then LiOH (1.1 equiv) was added. After 1 h, the mixture was quenched with water, acidified until pH 2 and extracted with ether. The combined organic layers were washed with saturated aqueous NH_4Cl solution, dried over $MgSO_4$ and evaporated under reduced pressure. Silica gel column chromatography purification (cyclohexane/EtOAc/AcOH, 7/3/0.1) afforded **22** as a white solid, 75% yield. R_f (cyclohexane/EtOAc: 4/1) 0.25; mp 117 °C; ^{1}H NMR ($CDCl_3$): δ 7.60 (d, *J* = 7.6 Hz, 1H); 7.22-7.29 (m, 5H); 7.17 (t, *J* = 7.1 Hz, 1H); 7.11 (t, *J* = 7.6 Hz, 1H); 7.07 (d, *J* = 7.1 Hz, 1H); 6.93 (s, 1H); 5.24 (s, 2H); 3.71 (t, *J* = 7.6 Hz, 2H); 2.76 (t, *J* = 7.6 Hz, 2H). ^{13}C NMR ($CDCl_3$): δ 179.5; 137.6; 136.7; 128.7; 127.7; 127.5; 126.7; 125.6; 121.9; 119.1; 118.8; 113.8; 109.7; 49.9; 34.8; 20.4. Anal. Calcd for $C_{18}H_{17}NO_2$: C, 77.40; H, 6.13; N, 5.01. Found: C, 77.12; H, 6.37; N, 4.89.

(*1R*)-*N*-3-(*N*-benzylindoylpropanoyl) camphorsultam (**23**): A solution of (+) 10,2-camphorsultam (1 equiv) in dimethoxyethane (3 mL.mmol^{-1}) was slowly added at room temperature to a suspension of sodium hydride (1.1 equiv) in the same solvent. The reaction mixture was stirred for 1 h. At the same time, isobutyl chloroformate and *N*-methylmorpholine (1.1 eq) were added to a solution of (*N*-benzylindoyl) propanoic acid **22** (1 equiv) in dimethoxyethane (3 mL.mmol^{-1}) cooled at -15°C. This solution was stirred for 15 min at -15°C, then filtered through a Celite pad under argon atmospher over the sultam sodium salt solution. The reaction mixture was stirred for 1 h at -15°C and 1 h at room temperature and then quenched with water, and concentrated. AcOEt was added and the organic layer was washed with aqueous NH_4Cl solution, dried over $MgSO_4$ and evaporated under reduced pressure. The compound was obtained by precipitation in an ether-pentane mixture. Silica gel column chromatography purification (cyclohexane/EtOAc/NEt_3, 8/2/0.1) afforded **23** as a white solid, 70% yield. R_f

(cyclohexane/EtOAc/NEt_3: 8/2/0.1) 0.42; mp 123 °C; $[\alpha]_D^{20}$ 57 (c 1. $CHCl_3$); ^{1}H NMR ($CDCl_3$): δ 7.63-7.65 (m, 1H); 7.20-7.28 (m, 4H); 7.07-7.16 (m, 4H); 6.97 (s, 1H); 5.23 (s, 2H); 3.85 (t, *J* = 6.3 Hz, 1H); 3.45 (d, *J* = 13.9 Hz, 1H); 3.42 (d, *J* = 13.9 Hz, 1H); 3.06-3.19 (m, 4H); 2.03-2.05 (m, 2H); 1.81-1.87 (m, 3H); 1.29-1.39 (m, 2H); 1.05 (s, 3H); 0.92 (s, 3H); ^{13}C NMR ($CDCl_3$): δ 171.5; 137.7; 136.6; 128.7; 127.9; 127.4; 126.7; 125.8; 121.7; 119.1; 119.0; 113.8; 109.5; 65.2; 52.9; 49.8; 48.4; 47.7; 44.6; 38.5; 36.1; 32.8; 26.4; 20.7; 20.2; 19.8. Anal. Calcd for $C_{28}H_{32}N_2O_3S$: C, 70.56; H, 6.77; N, 5.88. Found: C, 70.31; H, 6.98; N, 5.67.

(1*R*)-*N*-(2-Dibenzylaminomethyl-3-*N*-benzylindoyl propanoyl) camphorsultam (**24**): Trimethylsilylsulfate (1.5 equiv) and then triethylamine (1.1 equiv) were added to a dichloromethane solution of the sulfonamide **23** (1 equiv, 1 mL.mmol^{-1}). The reaction mixture was stirred for 6 h at room temperature. A solution of a *N*,*N*-dibenzyliminium trifluoroacetate salt (1.1 equiv) in dichloromethane, freshly prepared from *N,N,N',N'*,tetrabenzyl-methanediamine was added and the reaction mixture was stirred for 15 min. A solution of TBAF in THF (1 mol.L^{-1}, 1 equiv) was added, and then water was added. Dichloromethane was evaporated under reduced pressure and the aqueous solution was extracted with ether. The organic layer was washed with saturated aqueous NH_4Cl solution, dried over $MgSO_4$ and evaporated under reduced pressure. Silica gel column chromatography purification (cyclohexane/EtOAc, 9/1) afforded **24**, 88% yield. R_f (Cyclohexane/EtOAc, 4/1) 0.35; mp 80–81 °C; $[\alpha]_D^{20}$ 25 (c 1. $CHCl_3$); ^{1}H NMR ($CDCl_3$): δ 7.78-7.80 (m, 1H); 7.09-7.34 (m, 16H); 6.99-7.01 (m, 2H); 6.85 (s, 1H); 5.20 (s, 2H); 3.88 (m, 2H); 3.42-3.52 (m, 6H); 3.21 (dd, *J* = 14.4 Hz, 3.8 Hz, 1H); 2.94 (dd, *J* = 12.4 Hz, 10.3 Hz, 1H); 2.86 (dd, *J* = 14.4 Hz, 9.1 Hz, 1H); 2.56 (dd, *J* = 12.6 Hz, 4.5 Hz, 1H); 2.06-2.15 (m, 2H); 1.85-1.87 (m, 3H); 1.30-1.37 (m, 2H); 1.23 (s, 3H); 0.96 (s, 3H). ^{13}C NMR ($CDCl_3$): δ 174.7; 138.7; 137.9; 136.6; 129.1; 128.6; 128.4; 127.9; 127.0;

126.7; 126.6; 121.6; 119.6; 112.4; 109.4; 65.4; 57.5; 55.8; 53.2; 49.8; 48.3; 47.7; 44.7; 38.6; 32.8; 26.5; 25.8; 21.0; 19.9. Anal. Calcd for $C_{43}H_{47}N_3O_3S$: C, 75.29; H, 6.91; N, 6.13. Found: C, 75.45; H, 7.20; N, 5.81.

(*R*)-(*N-tert*-butyloxycarbonylaminomethyl)-3-*N*-benzylindolylpropanoic acid (**25**): $Pd(OH)_2$/C 20% (200 mg.mmol^{-1}) was added to a THF-MeOH (1/1, 5 mL.mmol^{-1}) solution of camphorsultam. The reaction mixture was stirred at room temperature under 5 bars hydrogen for 67 h. The solution was filtered through a Celite pad and then concentrated. The crude residue was dissolved in acetonitrile-H_2O (1/1, 5 mL.mmol-1). LiOH (2 equiv) was added and the reaction mixture was stirred overnight at room temperature. Acetonitrile was removed under reduced pressure and the aqueous layer was extracted once with ether. Dioxane (2.5 mL.mmol^{-1}), Boc_2O (1.2 equiv) and LiOH (pH = 9) were then added. The reaction mixture was stirred for 24 h, then acidified at pH = 2 at 0°C with HCl 1M and extracted with AcOEt. The organic layer was washed with saturated brine, dried over $MgSO_4$ and evaporated under reduced pressure. Silica gel column chromatography purification (cyclohexane/EtOAc/NEt3, 7/3/0.1) afforded **25**, 65% yield. ^{1}H NMR ($CDCl_3$): δ 7.62-6.98 (m, 10H); 6.62 (br, 0.5H); 5.27 (s, 2H); 4.96 (br, 0.5H); 3.43-3.30 (m, 2H); 3.21-2.84 (m, 3H); 1.43 and 1.25 (2s, 9H); ^{13}C NMR ($CDCl_3$): δ 179.9; 178.6; 158.1; 156.08; 137.7; 136.8; 136.6; 129.1; 128.8; 128.3; 128.1; 127.9; 127.6; 127.0; 126.7; 126.6; 125.4; 121.9; 119.3; 118.9; 111.6; 111.4; 109.9; 81.1; 79.7; 50.0; 46.8; 46.5; 42.6; 41.3; 28.4; 28.1; 25.7; 25.2.

2(*R*)-(1,3-Dihydro-1,3-dioxo-2*H*-isoindol-2-yl)-3-(1*H*-indole-3-yl)-propanoic acid, α-(aminomethyl)- (**12*R***): To a solution of *N-tert*-butyloxycarbonylaminomethyl-3-*N*-benzylindolylpropanoic acid **25** in THF (3 mL/mmol) were added the sodium (5 equiv) and liquid ammonia at -70°C. The blue solution was stirred for 1h at -50°C. After evaporation of

ammonia at room temperature, EtOAc and the saturated aqueous solution of NH_4Cl were added. Upon extraction with EtOAc, the combined extracts were washed with the saturated aqueous solution of NaCl, dried over $MgSO_4$ and then concentrated in vacuo leading to Boc-protected amino acid. The compound was obtained after flash column chromatography (Cy/EtOAc/AcOH, 7/3/1) as white powder, 48% yield. The compound was then treated with 1 mL TFA in 1 mL CH_2Cl_2 leading to the compound **26**. The compound **12** was obtained following the same procedure as for compound **2** using the compound **26** as amino acid. The product is isolated by preparative reverse phase HPLC, on a Symmetry, C8 (250 x 10 mm; 5µm) column with a multiple gradient of acetonitrile in water (20 to 40% during 5 min, 40 to 45 % during 20 min) at a flow rate of 3 mL/min. Light yellow solid, 11% yield. HPLC Rt = 18.5 min; ^{1}H-NMR ($CDCl_3$): δ (ppm) 7.81 (dd, *J* = 5.5 Hz, *J* = 3.1 Hz, 2H) ; 7.71 (dd, *J* = 5.5 Hz, *J* = 3.1 Hz, 2H); 7.62 (d, *J* = 7.7 Hz, 1H); 7.32 (d, *J* = 7.9 Hz, 1H); 7.18 (td, *J* = 8.1 Hz, *J* = 7.0 Hz, 1H); 7.15 (s, 1H); 7.12 (td, *J* = 1.08 Hz, *J* = 8.1 Hz, *J* = 7.0 Hz, 1H); 4.12 (dd, *J* = 14.0 Hz, *J* = 8.4 Hz, 1H); 3.98 (dd, *J* = 13.8 Hz, *J* = 5.9 Hz, 1H); 3.48 (m, 1H); 3.25 (dd, *J* = 15.1 Hz, *J* = 7.7 Hz, 1H); 3.09 (dd, *J* = 15.6 Hz, *J* = 6.8 Hz, 1H). ^{13}C-NMR ($CDCl_3$): δ (ppm) 176.2; 167.1; 135.1; 133; 130.8; 126.5; 126.2; 122.3; 121.5; 121.1; 118.5; 117.7; 110.9; 110.1; 109.9; 43.3; 38.4; 28.7. HRMS calcd for $C_{20}H_{16}N_2O_4$ [MH^+]: 349.1183. Found: 349.1181

2(*S*)-(1,3-Dihydro-1,3-dioxo-2*H*-isoindol-2-yl)-3-(1*H*-indole-3-yl)-propanoic acid, α-(aminomethyl)- (12*S*): ^{1}H-NMR (MeOD): δ (ppm) 7.82 (dd, *J* = 5.7 Hz, *J* = 3.1 Hz, 2H); 7.72 (dd, *J* = 5.5 Hz, *J* = 3 Hz, 2H); 7.62 (d, *J* = 7.6 Hz, 1H); 7.32 (d, *J* = 8.1 Hz, 2H); 7.19 (dd, *J* = 7.8 Hz, *J* = 6.8 Hz, 1H); 7.17 (s, 1H); 7.12 (dd, *J* = 8.8 Hz, *J* = 6.7 Hz, 1H); 7.13 (dd, *J* = 7.4 Hz, J = 6.7 Hz, 1H); 4.13 (dd, *J* = 13.8 Hz, *J* = 8.3 Hz, 1H); 3.99 (dd, *J* = 13.8 Hz, *J* = 5.9 Hz, 1H); 3.49 (m, 1H); 3.26 (dd, *J* = 14.9 Hz, *J* = 7.7 Hz, 1H); 3.10 (dd, *J* = 15.1 Hz, *J* = 6.6 Hz, 1H). ^{13}C-

NMR (MeOD): δ (ppm) 178.1; 168.1; 133.9; 131.8; 129.1; 123.3; 122.5; 122.1; 119.5; 118.7; 111.1; 44.2; 39.4; 32.7. HRMS calcd for $C_{20}H_{16}N_2O_4$ [MH^+]: 349.1183. Found: 349.1181

***N*-[2-(1,3-dihydro-1,3-dioxo-2*H*-isoindol-2-yl)acetyl]-L-tryptophan phenylmethyl ester** (**27**): *N*-Methyl morpholine (1.2 equiv) and isobutyl chloroformate (1.2 equiv) were successively added to a solution of *N*-phthaloylglycine (1.2 equiv) in THF (3 mL) at -20°C. After an activation period of 10 min, L-tryptophane benzyl ester (250 mg) in THF (2 mL) was added to above solution, and the resulting solution was stirred for 1h at -20°C prior to the addition of 5% $NaHCO_3$ (20 mL). After 30 min at room temperature, the aqueous phase was extracted with CH_2Cl_2 (3x50 mL). The combined organic layer were washed with 5 % $NaHCO_3$ (2x20 mL) and dried over Na_2SO_4. After evaporation under reduced pressure and purification by flash chromatography (EtOAc/ cyclohexane) (1/9), **27** was obtained as a white solid, 78 % yield; ^{1}H-NMR ($CDCl_3$): δ (ppm) 8.15 (s, 1H); 7.85 (m, 2H); 7.75 (m, 2H); 7.52 (d, *J* = 7.2 Hz, 1H); 7.37 (m, 3H); 7.28 (m, 3H); 7.11 (m, 2H); 6.80 (d, *J* = 2.3 Hz, 1H); 6.45 (d, *J* = 7.7 Hz, 1H); 5.11 (t, *J* = 12.3 Hz, 2H); 5.0 (m, 1H); 4.36 (d, *J* = 16.2 Hz, 1H); 4.26 (d, *J* = 16.2 Hz, 1H); 3.36 (m, 2H). ^{13}C-NMR ($CDCl_3$): δ (ppm) 171.3; 167.7; 165.7; 135.9; 135.1; 134.1; 131.9; 128.6; 128.5; 127.6; 123.6; 123.3; 122.1; 119.8; 118.5; 111.2; 109.3; 67.4; 53.4; 40.5; 27.4. HRMS: calcd for $C_{28}H_{23}N_3NaO_5$ [MNa^+]: 504.1529. Found: 504.1519

***N*-[2-(1,3-dihydro-1,3-dioxo-2*H*-isoindol-2-yl)acetyl]-L-tryptophan** (**14**): The compound **27** (70 mg) was dissolved in THF (8 mL) and the Pd/C 10% (0.1 equiv) was added. The mixture was stirred under hydrogen atmosphere for 48h. The solution was filtered from Pd/C and concentrated in vacuo. The product was purified by preparative reverse phase HPLC, on a Symmetry, C8 (250 x 10 mm; 5µm) column with a multiple gradient of acetonitrile in water (20 to 40% during 5 min, 40 to 45 % during 20 min) at a flow rate of 3 mL/min. White solid, 60%

yield; HPLC Rt = 11.2 min. ^{1}H-NMR (MeOD): δ (ppm) 7.87 (m, 2H); 7.81 (m, 2H); 7.56 (d, *J* = 6.8 Hz, 1H); 7.31 (d, *J* = 7 Hz, 1H); 7.12 (s, 1H); 7.06 (m, 2H); 4.72 (m, 1H); 4.35 (d, *J* = 16.6 Hz, 1H); 4.30 (d, *J* = 16.6 Hz, 1H); 3.35 (dd, 1H, *J* = 14.6 Hz, *J* = 6.6 Hz); 3.26 (dd, 1H, *J* = 14.1 Hz, *J* = 7 Hz). ^{13}C-NMR (MeOD): δ (ppm) 133.5; 123.1; 120.7; 117.7; 111.1; 53.8; 48.1; 39.6. HRMS calcd for $C_{21}H_{17}N_3NaO_5$ [MNa^+]: 414.1060. Found: 414.1059.

***tert*-Butyl 3-(((2*S*,3*R*)-2-(Benzyloxycarbonyl)-1-((*S*)-1-phenylethyl)pyrrolidin-3-yl)methyl)-1H-indole-1-carboxylate** (**29**): LDA (12 mL, 24 mmol) was added at -78 °C to a solution of (*S*)-benzyl 2-(but-3-enyl(1-phenylethyl)amino)acetate **28** (6.47 g, 20 mmol) in dry THF (30 mL) under argon. $ZnBr_2$ (1.2 M in Et_2O, 50 mL) was then added at the same temperature. The reaction mixture was stirred overnight at room temperature under argon. *tert*-Butyl 3-iodo-1H-indole-1-carboxylate (8.92 g, 26 mmol) in dry THF (10 mL), $Pd(OAc)_2$ (180 mg, 0.80 mmol), and *t*Bu_3P-HBF_4 (290 mg, 1.0 mmol) were then successively added, and the mixture was stirred overnight at room temperature under argon. Et_2O was added, and the organic layer was washed with NH_4Cl, dried over $MgSO_4$, and concentered in vacuo. The residue was purified by flash chromatography (cyclohexane/ethyl acetate 95:5) to give a yellow oil, 60% yield. $[\alpha]_D^{20}$ -37.9 (c 1, $CHCl_3$). ^{1}H NMR ($CDCl_3$) δ 8.09 (d, 1H, *J* = 8.0 Hz), 7.38-7.16 (m, 14H), 5.10 (AB, 2H, *J* = 12 Hz), 3.73 (q, 1H, *J* = 6.8 Hz), 3.55 (d, 1H, *J* = 7.7 Hz), 3.09 (m, 1H), 2.91 (m, 1H), 2.81-2.73 (m, 2H), 2.36 (m, 1H), 1.92 (m, 1H), 1.76 (m, 1H), 1.64 (s, 9H), 1.35 (d, 3H, *J* = 6.8 Hz). ^{13}C NMR ($CDCl_3$) δ 173.2, 149.8, 144.5, 135.9, 135.5, 130.5, 128.9, 128.6, 128.4, 127.5, 127.2, 124.4, 122.8, 122.4, 119.0, 115.3, 83.5, 66.7, 66.0, 61.6, 50.1, 41.8, 30.2, 28.3, 26.4, 22.9. HRMS calcd for $C_{34}H_{38}N_2O_4$ [MH^+]: 539.2904. Found: 539.2910.

(2*S*, 3*R*)-3-((1-(*tert*-Butoxycarbonyl)-1*H*-indol-3-yl)methyl)pyrrolidine-2 carboxylic acid (**30**): **29** (8.056 mmol, 4.34 g) was dissolved in MeOH (60 mL) and Pd/C 10% (1.2 g) was

added. The mixture was stirred under 5 bar hydrogen for one week. The solution was filtered over Celite and concentrated. The residue was purified by flash chromatography (CH_2Cl_2/MeOH 9:1) to give an oil, 79% yield. ^{1}H-NMR ($CDCl_3$): δ (ppm) 8.07 (s, 1H); 7.52 (d, *J* = 7.6 Hz, 1H); 7.38 (s, 1H); 7.24 (t, *J* = 7.9 Hz, 1H); 7.10 (t, J = 7.3 Hz, 1H); 4.40 (m, 1H); 3.83 (m, 2H); 3.12 (d, *J* = 12 Hz,1H); 2.99 (m, 1H); 2.67 (t, *J* = 12 Hz, 1H); 1.98 (m, 1H); 1.87 (m, 1H); 1.61 (s, 9H); ^{13}C-NMR ($CDCl_3$): δ (ppm) 172.2; 149.8; 135.6; 130.4; 124.5; 123.5; 122.7; 118.1; 115.4; 110.1; 83.7; 64.6; 44.8; 40.8; 29.4; 28.3; 24.6. HRMS calcd for $C_{19}H_{24}N_2O_4Na$ [MNa^+]: 367.1628 Found: 367.1628

(2*S*,3*R*)-3-((1*H*-indol-3-yl)methyl)-1-(2-(1,3-dioxoisoindolin-2-yl)acetyl)pyrrolidine-2-carboxylic acid (**15**): The compound **30** (1 mmol, 360 mg) was dissolved in DMF (1 mL) under N_2, to the solution were added the HATU (1 equiv) and DIPEA (1 equiv), the mixture was stirred for 20 min and the *N*-phthaloylglycine (1.2 equiv) was added. After stirring the mixture overnight, EtOAc (20 mL) was added. The organic layer was washed with saturated $NaHCO_3$ (2 x 20 mL) and 10% aqueous citric acid (2 x 20 mL), dried with Na_2SO_4, filtered and concentrated. The crude residue was dissolved in TFA (3 mL) and the mixture was stirred at room temperature for 4 h. TFA was co-evaporated with cyclohexane and the crude residue was purified by preparative reverse phase HPLC, on a Symmetry, C8 (250 x 10 mm; 5µm) column with a multiple gradient of acetonitrile in water (20 to 40% during 5 min, 40 to 45 % during 20 min) at a flow rate of 3 mL/min. Compound **15** was obtained as a light yellow solid, 20% yield; HPLC Rt = 13.5 min; ^{1}H-NMR (DMSO): δ (ppm) 7.92 (m, 4H); 7.55 (d, 1H, *J* = 7.6 Hz); 7.36 (d, 1H, *J* = 8.1 Hz); 7.23 (s, 1H); 7.09 (dd, 1H, *J* = 8.1 Hz, *J* = 7.8 Hz); 6.99 (dd, 1H, *J* = 7.8 Hz, *J* = 7.5 Hz); 4.55 (d, 1H, *J* = 16.8 Hz); 4.42 (d, 1H, *J* = 8.1 Hz); 4.40 (d, 1H, *J* = 17 Hz); 3.85 (t, 2H, *J* = 8.3 Hz); 3.02 (dd, 1H, *J* = 14.2 Hz, *J* = 4.3 Hz); 2.78 (m, 1H); 2.46 (dd, 1H, *J* = 14.2 Hz, *J* = 4.1

Hz); 1.87 (m, 1H); ^{13}C-NMR (DMSO): δ (ppm) 171.9; 167.5; 164.2; 136.2; 134.7; 131.5; 126.9; 123.2; 122.9; 120.9; 118.2; 118.1; 112.1; 111.4; 83.5; 62.1; 45; 40.7; 38.4; 31; 28.7. HRMS calcd for $C_{24}H_{22}N_3O_5$ [MH^+]: 432.1554. Found: 432.1599

(2*S*,3*R*)-3-(1*H*-indol-3-yl)methyl)-1-(2-naphthoyl)pyrrolidine-2-carboxylic acid (**16**): **30** (1 mmol, 360 mg) was dissolved in CH_2Cl_2 (10 mL). NEt_3 (2.5 equiv) and naphthoyl chloride (2 equiv) were added successively. After stirring the mixture overnight at room temperature, the solvent was evaporated and the residue was dissolved in AcOEt and washed with NH_4Cl. The crude residue was dissolved in TFA (3 mL) and the mixture was stirred at room temperature for 4 h. TFA was co-evaporated with cyclohexane and the crude residue was purified by flash chromatography on silica gel (CH_2Cl_2/MeOH 9:1 with AcOH 0.1%) to afford **16** as a beige solid, 63% yield. HPLC Rt = 19.4 min. ^{1}H-NMR ($CDCl_3$): δ (ppm) 8.03 (s, 1H); 7.88 (m, 4H); 7.36 (d, 1H, *J* = 8.1 Hz); 7.23 (s, 1H); 7.09 (dd, 1H, *J* = 8.1 Hz, *J* = 7.8 Hz); 6.99 (dd, 1H, *J* = 7.8 Hz, *J* = 7.5 Hz); 4.55 (d, 1H, *J* = 16.8 Hz); 4.42 (d, 1H, *J* = 8.1 Hz); 4.40 (d, 1H, *J* = 17 Hz); 3.85 (t, 2H, *J* = 8.3 Hz); 3.02 (dd, 1H, *J* = 14.2 Hz, *J* = 4.3 Hz); 2.78 (m, 1H); 2.46 (dd, 1H, *J* = 14.2 Hz, *J* = 4.1 Hz); 1.87 (m, 1H); ^{13}C-NMR ($CDCl_3$): δ (ppm) 173.3; 157.8; 135.4; 132.4; 128.6; 128.3; 128.1; 127.8; 127.6; 126.8; 124.1; 122.7; 122.1; 119.5; 118.7; 112.5; 111.3; 64.4; 50.1; 42.7; 31; 27.8. HRMS calcd for $C_{25}H_{23}N_2O_3$ [MH^+]: 399.1703. Found: 399.1708

(2*S*,3*R*)-3-(1*H*-indol-3-yl)methyl)-1-benzoylpyrrolidine-2-carboxylic acid (**17**): **30** (1.25 mmol, 432 mg) was dissolved in CH_2Cl_2 (15 mL). NEt_3 (2.5 equiv) and benzoyl chloride (2 equiv) were added successively. After stirring the mixture for 4 h at room temperature, the solvent was evaporated and the residue was dissolved in AcOEt and washed with NH_4Cl. The crude residue was dissolved in TFA (3 mL) and the mixture was stirred at room temperature overnight. TFA was co-evaporated with cyclohexane and the crude residue was purified by flash

chromatography on silica gel (CH_2Cl_2/MeOH 9:1 with AcOH 0.1%) to afford **17** as a beige solid (387 mg, 67%). HPLC Rt = 21.4 min. ^{1}H-NMR ($CDCl_3$): δ (ppm) 8.13 (d, 1H); 7.66 (d, 1H, *J* = 8.1 Hz); 7.52 (m, 5H); 7.23 (t, 1H, *J* = 7 Hz); 7.16 (t, 1H, *J* = 6.8 Hz); 7.12 (s, 1H); 4.59 (d, 1H, *J* = 6.6 Hz); 3.61 (m, 2H); 3.23 (dd, 1H, *J* = 14.4 Hz, *J* = 5.5 Hz); 3.13 (m, 1H); 2.93 (dd, 1H, *J* = 14.2 Hz, *J* = 8.3 Hz); 2.09 (m, 1H); 1.74 (m, 1H); ^{13}C-NMR ($CDCl_3$): δ (ppm) 173.7; 171.8; 136.3; 134.6; 130.9; 128.5; 127.6; 127.3; 126.5; 122.7; 122.1; 119.6; 118.7; 112.6; 111.3; 64.3; 50; 42.8; 31; 27.7. HRMS calcd for $C_{21}H_{21}N_2O_3$ [MH^+]: 349.1547. Found: 349.1517

(2*S*,3*R*)-3-((1*H*-indol-3-yl)methyl)-1-((2,4-dinitrophenyl)thio)pyrrolidine-2-carboxylic acid (**18**): To a solution of **30** (1 mmol, 360 mg) in 2M NaOH (1 mL) and dioxane (5 mL), 2,4-dinitrophenylsulfenyl chloride (1.1 equiv) was added dropwise over 15 min, whilst 2M NaOH (2 mL) was added dropwise with vigorous stirring. The mixture was diluted with H_2O (50 mL), filtered from precipitated disulfide, overlayered with EtOAc and acidified with 0.5M H_2SO_4. Upon extraction with EtOAc, the combined extracts were washed twice with H_2O and then dried over Na_2SO_4. The crude residue was dissolved in TFA (3 mL) and the mixture was stirred at room temperature for 4 h. TFA was co-evaporated with cyclohexane and the crude residue was purified by HPLC in the same conditions as described above leading to **18** as a yellow solid, 55% yield. HPLC Rt = 21.9 min. ^{1}H-NMR (MeOD): δ (ppm) 9.13 (s, 1H); 8.46 (dd, 1H, *J* = 21 Hz, *J* = 9.4 Hz); 7.76 (dd, 1H, *J* = 15.6Hz, *J* = 9.4 Hz); 7.26 (dd, 1H, *J* = 6.8 Hz, *J* = 7.4 Hz); 7.15 (dd, 1H, *J* = 14.6 Hz, *J* = 7.2 Hz); 6.91 (d, 1H, *J* = 14.8 Hz); 6.91 (s, 1H); 6.78 (d, 1H, *J* = 7.8 Hz); 4.41 (dd, 1H, *J* = 8.9 Hz, *J* = 9.8 Hz); 3.65 (m, 2H); 2.78 (m, 1H); 2.37 (m, 1H); 2.13 (m, 1H); 1.89 (m, 2H); ^{13}C-NMR (MeOD): δ (ppm) 186.7; 170.4; 152.4; 146.7; 134; 131; 129.6; 128.7; 126.8; 125.7; 122.6; 122.1; 119.5; 110.1; 112.6; 63.9; 45.7; 40.4; 39.6; 30.5; 29.6. HRMS calcd for $C_{20}H_{19}N_4O_6SNa$ [MNa^+]: 465.0839. Found: 465.0839

C5 DNA methyltransferase activity assay.

The human DNMT1 was produced in H19 cells through the bacculovirus system as described in [27]. The enzyme was incubated at 350 nM in reaction buffer (20 mM HEPES pH 7.2, 50 mM KCl, 1 mM EDTA, 25 µg/mL BSA) in presence of 0.2 µM of the same hemimethylated DNA duplex (5′GAT^{Me}CGC^{Me}CGATG^{Me}CG^{Me}CGAAT^{Me}CG^{Me}CGAT^{Me}CGATG^{Me}CGAT3′/5′ATCGCATCGATCGCGATTCG CGCATCGGCGATC 3′) and of the tested compounds with 280 nM (0.15 µCi) methyl-^{3}H AdoMet and 1.28 µM unlabeled AdoMet in a total volume of 50 µL for 2h at 37°C. After incubation, the unincorporated AdoMet and the enzymes were removed with P-30 Tris Micro Bio-Spin Biospin chromatography columns (Biorad) and the incorporation of radioactivity was determined by liquid scintillation counting (Wallac Microbeta 1450 Trilux, Perkin Elmer). Background levels were determined in samples lacking the DNA substrate. The results were plotted as relative methylation activity (expressed in % normalized to samples in the absence of tested compounds) against the logarithm of the inhibitor concentration and fitted by non-linear regression with the GraphPad Prism™ software.

MTS assay

The DU145 cell line was maintained in RPMI (Invitrogen, France) supplemented with 10% foetal bovine serum (Perbio, Belgium) and 2 mM glutamine. Cells were incubated at 37°C in a humidified atmosphere of 5% CO_2 in air. $3x10^4$ DU145 cells were seeded in 96 well plates in 80 µL medium/well and incubated after seeding with 20 µL of increasing concentrations of inhibitor. Absorbance at 490 nm was determined after 72h of incubation upon use of CellTiter96

Aqueous Non-Radioactive Cell Proliferation Assay following the manufacturer's instructions (Promega, Germany).

NMR binding experiments. 1D ^{1}H spectra were recorded on a Bruker Avance III spectrometer operating at 500 MHz and equipped with a TCI cryoprobe. WaterLOGSY spectra were acquired at 25°C using a recycling delay of 2 s, a NOE mixing period of 1 s, and an acquisition time of 0.3 s, with 512 scans. Water resonance was selectively inverted using a Gaussian pulse of 20 ms duration. An excitation sculpting scheme incorporating selective 180° REBURP pulses of 3 ms length centered in the aromatic region was applied to suppress water resonance and signals in the aliphatic region arising from the buffer (20 mM HEPES, pH 7.4, 0.2 mM DTT, 1 mM EDTA, 200 mM KCl). The C-terminal catalytic domain of the murine Dnmt3A (623-908) was obtained as described in [58].

Docking analysis

The structure of murine Dnmt1 (residues 732-1600) resolved with AdoHcy and the DNA substrate was taken from Protein data bank (PDB) (4DA4). The SYBYL-X 1.3 software from Tripos (L.P., USA) was used for analysis and the images were prepared with Benchware 3D Explorer from Tripos (L.P., USA).

Preparation of Protein Structure: the protein structure was prepared using the Protein Preparation tool, biopolymer implemented, in Sybyl (version X 2.1, Certara) with the following steps: the missing side chains were added to the crystal structure, hydrogen atoms were added, protonation states of entire systems were adjusted to pH 7.4, water molecules outside 5Å of the co-crystallized ligands and ligands were removed, hydrogen bond networks and flip

orientations/tautomeric states of Gln, Asn and His residues were optimized and the geometry optimization was performed by a staged minimization with the MMF94 force field until the energy difference between iterations was lower than 0.05 kcal/mol.

IFD procedure: the complex structure of 4DA4 was used as a starting point for the IFD protocol implemented in the Surflex-Dock GeomX software suite, *i.e.* use of Surflex with the most exhaustive accuracy parameter set to dock the ligands.

The protonated ligands AdoHcy, **1**, compound 5 by Suzuki *et al*[38], novel compounds **16** and **17** were docked into the protein structure using the following steps: the receptor grid was defined as an enclosing box centered at the cocrystallized ligands (i.e., cytidine and AdoHcy) to include the cofactor and substrate binding sites, the protein movements were allowed for hydrogen and heavy atoms in the box. The most favorable binding conformations of each receptor and ligand complex were selected by the best docked poses. Figures show the top scored binding poses and schematic 2D representation of ligands as compared to the reference AdoHcy ligand.

Corresponding Authors

*Dominique Guianvarc'h: Phone: +33144275511; Fax: +33144276701; E-mail: dominique.guianvarch@upmc.fr.

*Paola B. Arimondo: Phone: +33534506492; Fax: +33534503492; E-mail : paola.arimondo@etac.cnrs.fr

Author Contributions

The manuscript was written through contributions of all authors. All authors have given approval to the final version of the manuscript.

ACKNOWLEDGMENT

This work was supported by ANR-06 JCJCJ-0080 to PBA and DG. CC was recipient of a CNRS-INSERM BDI and AC of an ARC fellowship. The authors thank Lionel Dubost and Dr. Arul Marie of the MNHN Mass Spectroscopy Service for mass spectra analysis, Prof. Philippe Grellier of the MNHN CNRS FRE 3206 for use of the microbeta counter, Prof William G. Nelson at John Hopkins University, Baltimore, USA, for the DNMT1 construction, Dr. Ahmed El Marjou at Institut Curie UMR144 CNRS for DNMT1 production and Prof Solange Lavielle at Université Pierre et Marie Curie-Paris 6 - ENS – CNRS UMR 7203 for helpful discussion.

ABBREVIATIONS

5-aza-C, 5-aza-cytidine; 5-aza-dC, 5-aza-deoxycytidine; AdoMet, *S*-adenosyl-L-methionine; AdoHcy, *S*-adenosyl-L-homocysteine; DNMT, DNA methyltransferase; IFD, Induced-Fit Docking; STD, saturation transfer difference.

Supporting Information Available: Supplementary figures of IFD of AdoHcy and compound **17** (2*R*, 3*S*) in the three-dimensional structure of the catalytic murine Dnmt1 (residues 732-1600) (from PDB 4DA4). This material is available free of charge via the Internet at http://pubs.acs.org.

REFERENCES

(1) Berger, S. L.; Kouzarides, T.; Shiekhattar, R.; Shilatifard, A. An operational definition of epigenetics. *Genes Dev.* **2009**, *23*, 781–783.

(2) Illingworth, R. S.; Bird, A. P. CpG islands--'a rough guide'. *FEBS Lett.* **2009**, *583*, 1713–1720.

(3) Weber, M.; Hellmann, I.; Stadler, M. B.; Ramos, L.; Pääbo, S.; Rebhan, M.; Schübeler, D. Distribution, silencing potential and evolutionary impact of promoter DNA methylation in the human genome. *Nat. Genet.* **2007**, *39*, 457–466.

(4) Esteller, M. Epigenetics in cancer. *N. Engl. J. Med.* **2008**, *358*, 1148–1159.

(5) Feinberg, A. P. Phenotypic plasticity and the epigenetics of human disease. *Nature* **2007**, *447*, 433–440.

(6) Portela, A.; Esteller, M. Epigenetic modifications and human disease. *Nat. Biotechnol.* **2010**, *28*, 1057–1068.

(7) Kelly, T. K.; De Carvalho, D. D.; Jones, P. A. Epigenetic modifications as therapeutic targets. *Nat. Biotechnol.* **2010**, *28*, 1069–1078.

(8) Greger, V.; Passarge, E.; Höpping, W.; Messmer, E.; Horsthemke, B. Epigenetic changes may contribute to the formation and spontaneous regression of retinoblastoma. *Hum. Genet.* **1989**, *83*, 155–158.

(9) Baylin, S. B.; Herman, J. G. Promoter hypermethylation--can this change alone ever designate true tumor suppressor gene function? *J. Natl. Cancer Inst.* **2001**, *93*, 664–665.

(10) Jones, P. A.; Baylin, S. B. The Epigenomics of Cancer. *Cell* **2007**, *128*, 683–692.

(11) Jurkowska, R. Z.; Jurkowski, T. P.; Jeltsch, A. Structure and function of mammalian

DNA methyltransferases. *Chembiochem* **2011**, *12*, 206–222.

(12) Yu, N.; Wang, M. Anticancer drug discovery targeting DNA hypermethylation. *Curr. Med. Chem.* **2008**, *15*, 1350–1375.

(13) Szyf, M. Epigenetics, DNA methylation, and chromatin modifying drugs. *Annu. Rev. Pharmacol. Toxicol.* **2009**, *49*, 243–263.

(14) Mai, A.; Altucci, L. Epi-drugs to fight cancer: from chemistry to cancer treatment, the road ahead. *Int. J. Biochem. Cell Biol.* **2009**, *41*, 199–213.

(15) Stresemann, C.; Lyko, F. Modes of action of the DNA methyltransferase inhibitors azacytidine and decitabine. *Int. J. Cancer* **2008**, *123*, 8–13.

(16) Juergens, R. A.; Wrangle, J.; Vendetti, F. P.; Murphy, S. C.; Zhao, M.; Coleman, B.; Sebree, R.; Rodgers, K.; Hooker, C. M.; Franco, N.; Lee, B.; Tsai, S.; Delgado, I. E.; Rudek, M. A.; Belinsky, S. A.; Herman, J. G.; Baylin, S. B.; Brock, M. V.; Rudin, C. M. Combination Epigenetic Therapy Has Efficacy in Patients with Refractory Advanced Non–Small Cell Lung Cancer. *Cancer Discovery* **2011**, *1*, 598–607.

(17) Chuang, J. C.; Warner, S. L.; Vollmer, D.; Vankayalapati, H.; Redkar, S.; Bearss, D. J.; Qiu, X.; Yoo, C. B.; Jones, P. A. S110, a 5-Aza-2'-deoxycytidine-containing dinucleotide, is an effective DNA methylation inhibitor in vivo and can reduce tumor growth. *Mol. Cancer Ther.* **2010**, *9*, 1443–1450.

(18) Chuang, J. C.; Yoo, C. B.; Kwan, J. M.; Li, T. W. H.; Liang, G.; Yang, A. S.; Jones, P. A. Comparison of biological effects of non-nucleoside DNA methylation inhibitors versus 5-aza-2'-deoxycytidine. *Mol. Cancer Ther.* **2005**, *4*, 1515–1520.

(19) Rajavelu, A.; Tulyasheva, Z.; Jaiswal, R.; Jeltsch, A.; Kuhnert, N. The inhibition of the mammalian DNA methyltransferase 3a (Dnmt3a) by dietary black tea and coffee polyphenols.

BMC Biochem. **2011**, *12*, 16.

(20) Fang, M. Z.; Wang, Y.; Ai, N.; Hou, Z.; Sun, Y.; Lu, H.; Welsh, W.; Yang, C. S. Tea Polyphenol (−)-Epigallocatechin-3-Gallate Inhibits DNA Methyltransferase and Reactivates Methylation-Silenced Genes in Cancer Cell Lines. *Cancer Res* **2003**, *63*, 7563–7570.

(21) Fang, M. Z.; Chen, D.; Sun, Y.; Jin, Z.; Christman, J. K.; Yang, C. S. Reversal of Hypermethylation and Reactivation of p16INK4a, RARβ, and MGMT Genes by Genistein and Other Isoflavones from Soy. *Clin Cancer Res* **2005**, *11*, 7033–7041.

(22) Kuck, D.; Caulfield, T.; Lyko, F.; Medina-Franco, J. L. Nanaomycin A selectively inhibits DNMT3B and reactivates silenced tumor suppressor genes in human cancer cells. *Mol. Cancer Ther.* **2010**, *9*, 3015–3023.

(23) Piña, I. C.; Gautschi, J. T.; Wang, G.-Y.-S.; Sanders, M. L.; Schmitz, F. J.; France, D.; Cornell-Kennon, S.; Sambucetti, L. C.; Remiszewski, S. W.; Perez, L. B.; Bair, K. W.; Crews, P. Psammaplins from the sponge Pseudoceratina purpurea: inhibition of both histone deacetylase and DNA methyltransferase. *J. Org. Chem.* **2003**, *68*, 3866–3873.

(24) Fagan, R. L.; Cryderman, D. E.; Kopelovich, L.; Wallrath, L. L.; Brenner, C. Laccaic Acid A Is a Direct, DNA-competitive Inhibitor of DNA Methyltransferase 1. *J. Biol. Chem.* **2013**, *288*, 23858–23867.

(25) Singh, N.; Dueñas-González, A.; Lyko, F.; Medina-Franco, J. L. Molecular Modeling and Molecular Dynamics Studies of Hydralazine with Human DNA Methyltransferase 1. *ChemMedChem* **2009**, *4*, 792–799.

(26) Villar-Garea, A.; Fraga, M. F.; Espada, J.; Esteller, M. Procaine is a DNA-demethylating agent with growth-inhibitory effects in human cancer cells. *Cancer Res.* **2003**, *63*, 4984–4989.

(27) Lee, B. H.; Yegnasubramanian, S.; Lin, X.; Nelson, W. G. Procainamide is a specific

inhibitor of DNA methyltransferase 1. *J. Biol. Chem.* **2005**, *280*, 40749–40756.

(28) Kuck, D.; Singh, N.; Lyko, F.; Medina-Franco, J. L. Novel and selective DNA methyltransferase inhibitors: Docking-based virtual screening and experimental evaluation. *Bioorg. Med. Chem.* **2010**, *18*, 822–829.

(29) Medina-Franco, J. L.; López-Vallejo, F.; Kuck, D.; Lyko, F. Natural products as DNA methyltransferase inhibitors: a computer-aided discovery approach. *Mol. Divers.* **2011**, *15*, 293–304.

(30) Brueckner, B.; Boy, R. G.; Siedlecki, P.; Musch, T.; Kliem, H. C.; Zielenkiewicz, P.; Suhai, S.; Wiessler, M.; Lyko, F. Epigenetic Reactivation of Tumor Suppressor Genes by a Novel Small-Molecule Inhibitor of Human DNA Methyltransferases. *Cancer Res* **2005**, *65*, 6305–6311.

(31) Stresemann, C.; Brueckner, B.; Musch, T.; Stopper, H.; Lyko, F. Functional diversity of DNA methyltransferase inhibitors in human cancer cell lines. *Cancer Res.* **2006**, *66*, 2794–2800.

(32) Datta, J.; Ghoshal, K.; Denny, W. A.; Gamage, S. A.; Brooke, D. G.; Phiasivongsa, P.; Redkar, S.; Jacob, S. T. A new class of quinoline-based DNA hypomethylating agents reactivates tumor suppressor genes by blocking DNA methyltransferase 1 activity and inducing its degradation. *Cancer Res.* **2009**, *69*, 4277–4285.

(33) Isakovic, L.; Saavedra, O. M.; Llewellyn, D. B.; Claridge, S.; Zhan, L.; Bernstein, N.; Vaisburg, A.; Elowe, N.; Petschner, A. J.; Rahil, J.; Beaulieu, N.; Gauthier, F.; MacLeod, A. R.; Delorme, D.; Besterman, J. M.; Wahhab, A. Constrained (l-)-S-adenosyl-l-homocysteine (SAH) analogues as DNA methyltransferase inhibitors. *Bioorg. Med. Chem. Lett.* **2009**, *19*, 2742–2746.

(34) Saavedra, O. M.; Isakovic, L.; Llewellyn, D. B.; Zhan, L.; Bernstein, N.; Claridge, S.; Raeppel, F.; Vaisburg, A.; Elowe, N.; Petschner, A. J.; Rahil, J.; Beaulieu, N.; MacLeod, A. R.;

Delorme, D.; Besterman, J. M.; Wahhab, A. SAR around (l)-S-adenosyl-l-homocysteine, an inhibitor of human DNA methyltransferase (DNMT) enzymes. *Bioorg. Med. Chem. Lett.* **2009**, *19*, 2747–2751.

(35) Gros, C.; Fahy, J.; Halby, L.; Dufau, I.; Erdmann, A.; Gregoire, J.-M.; Ausseil, F.; Vispé, S.; Arimondo, P. B. DNA methylation inhibitors in cancer: recent and future approaches. *Biochimie* **2012**, *94*, 2280–2296.

(36) Ceccaldi, A.; Rajavelu, A.; Champion, C.; Rampon, C.; Jurkowska, R.; Jankevicius, G.; Sénamaud-Beaufort, C.; Ponger, L.; Gagey, N.; Ali, H. D.; Tost, J.; Vriz, S.; Ros, S.; Dauzonne, D.; Jeltsch, A.; Guianvarc'h, D.; Arimondo, P. B. C5-DNA methyltransferase inhibitors: from screening to effects on zebrafish embryo development. *Chembiochem* **2011**, *12*, 1337–1345.

(37) Halby, L.; Champion, C.; Sénamaud-Beaufort, C.; Ajjan, S.; Drujon, T.; Rajavelu, A.; Ceccaldi, A.; Jurkowska, R.; Lequin, O.; Nelson, W. G.; Guy, A.; Jeltsch, A.; Guianvarc'h, D.; Ferroud, C.; Arimondo, P. B. Rapid synthesis of new DNMT inhibitors derivatives of procainamide. *Chembiochem* **2012**, *13*, 157–165.

(38) Suzuki, T.; Tanaka, R.; Hamada, S.; Nakagawa, H.; Miyata, N. Design, synthesis, inhibitory activity, and binding mode study of novel DNA methyltransferase 1 inhibitors. *Bioorg. Med. Chem. Lett.* **2010**, *20*, 1124–1127.

(39) Castellano, S.; Kuck, D.; Sala, M.; Novellino, E.; Lyko, F.; Sbardella, G. Constrained Analogues of Procaine as Novel Small Molecule Inhibitors of DNA Methyltransferase-1. *J. Med. Chem.* **2008**, *51*, 2321–2325.

(40) Castellano, S.; Kuck, D.; Viviano, M.; Yoo, J.; López-Vallejo, F.; Conti, P.; Tamborini, L.; Pinto, A.; Medina-Franco, J. L.; Sbardella, G. Synthesis and biochemical evaluation of δ(2)-isoxazoline derivatives as DNA methyltransferase 1 inhibitors. *J. Med. Chem.* **2011**, *54*, 7663–

7677.

(41) Casimir, J. R.; Guichard, G.; Briand, J.-P. Methyl 2-((succinimidooxy)carbonyl)benzoate (MSB): a new, efficient reagent for N-phthaloylation of amino acid and peptide derivatives. *J. Org. Chem.* **2002**, *67*, 3764–3768.

(42) Canonne, P.; Akssira, M.; Dahdouh, A.; Kasmi, H.; Boumzebra, M. Synthesis of Chiral 3-Substituted 2,4(1H,3H)-Quinazolinediones. *HETEROCYCLES* **1993**, *36*, 1305.

(43) Moumne, R.; Larregola,, M.; Boutadla,, M.; Karoyan, P. Aminomethylation of chiral silyl enol ethers; access to beta(2)-homotryptophane and beta(2)-homolysine derivatives. *Tethradron Letters* **2009**, *49*, 4704–4706.

(44) Mothes, C.; Lavielle, S.; Karoyan, P. Amino-Zinc-Ene-Enolate Cyclization: A Short Access to cis-3-Substituted Prolino-homotryptophane Derivatives. *J. Org. Chem.* **2008**, *73*, 6706–6710.

(45) Siedlecki, P.; Garcia Boy, R.; Musch, T.; Brueckner, B.; Suhai, S.; Lyko, F.; Zielenkiewicz, P. Discovery of two novel, small-molecule inhibitors of DNA methylation. *J. Med. Chem.* **2006**, *49*, 678–683.

(46) Siedlecki, P.; Garcia Boy, R.; Comagic, S.; Schirrmacher, R.; Wiessler, M.; Zielenkiewicz, P.; Suhai, S.; Lyko, F. Establishment and functional validation of a structural homology model for human DNA methyltransferase 1. *Biochem. Biophys. Res. Commun.* **2003**, *306*, 558–563.

(47) Baud, M. G. J.; Leiser, T.; Haus, P.; Samlal, S.; Wong, A. C.; Wood, R. J.; Petrucci, V.; Gunaratnam, M.; Hughes, S. M.; Buluwela, L.; Turlais, F.; Neidle, S.; Meyer-Almes, F.-J.; White, A. J. P.; Fuchter, M. J. Defining the mechanism of action and enzymatic selectivity of psammaplin A against its epigenetic targets. *J. Med. Chem.* **2012**, *55*, 1731–1750.

(48) Dalvit, C.; Pevarello, P.; Tatò, M.; Veronesi, M.; Vulpetti, A.; Sundström, M. Identification of compounds with binding affinity to proteins via magnetization transfer from bulk water. *J. Biomol. NMR* **2000**, *18*, 65–68.

(49) Dalvit, C.; Fogliatto, G.; Stewart, A.; Veronesi, M.; Stockman, B. WaterLOGSY as a method for primary NMR screening: practical aspects and range of applicability. *J. Biomol. NMR* **2001**, *21*, 349–359.

(50) Dalvit, C. Theoretical analysis of the competition ligand-based NMR experiments and selected applications to fragment screening and binding constant measurements. *Concepts in Magnetic Resonance Part A* **2008**, *32A*, 341–372.

(51) Schirrmacher, E.; Beck, C.; Brueckner, B.; Schmitges, F.; Siedlecki, P.; Bartenstein, P.; Lyko, F.; Schirrmacher, R. Synthesis and in vitro evaluation of biotinylated RG108: a high affinity compound for studying binding interactions with human DNA methyltransferases. *Bioconjug. Chem.* **2006**, *17*, 261–266.

(52) Song, J.; Teplova, M.; Ishibe-Murakami, S.; Patel, D. J. Structure-Based Mechanistic Insights into DNMT1-Mediated Maintenance DNA Methylation. *Science* **2012**, *335*, 709–712.

(53) Rathert, P.; Cheng, X.; Jeltsch, A. Continuous enzymatic assay for histone lysine methyltransferases. *BioTechniques* **2007**, *43*, 602, 604, 606 passim.

(54) Urig, S.; Gowher, H.; Hermann, A.; Beck, C.; Fatemi, M.; Humeny, A.; Jeltsch, A. The Escherichia coli dam DNA methyltransferase modifies DNA in a highly processive reaction. *J. Mol. Biol.* **2002**, *319*, 1085–1096.

(55) Horton, J. R.; Liebert, K.; Hattman, S.; Jeltsch, A.; Cheng, X. Transition from nonspecific to specific DNA interactions along the substrate-recognition pathway of dam methyltransferase. *Cell* **2005**, *121*, 349–361.

(56) Liebert, K.; Horton, J. R.; Chahar, S.; Orwick, M.; Cheng, X.; Jeltsch, A. Two alternative conformations of S-adenosyl-L-homocysteine bound to Escherichia coli DNA adenine methyltransferase and the implication of conformational changes in regulating the catalytic cycle. *J. Biol. Chem.* **2007**, *282*, 22848–22855.

(57) Roth, M.; Jeltsch, A. Biotin-avidin microplate assay for the quantitative analysis of enzymatic methylation of DNA by DNA methyltransferases. *Biol. Chem.* **2000**, *381*, 269–272.

(58) Jia, D.; Jurkowska, R. Z.; Zhang, X.; Jeltsch, A.; Cheng, X. Structure of Dnmt3a bound to Dnmt3L suggests a model for de novo DNA methylation. *Nature* **2007**, *449*, 248–251.

FIGURES

Figure 1. Inhibitors of DNMTs

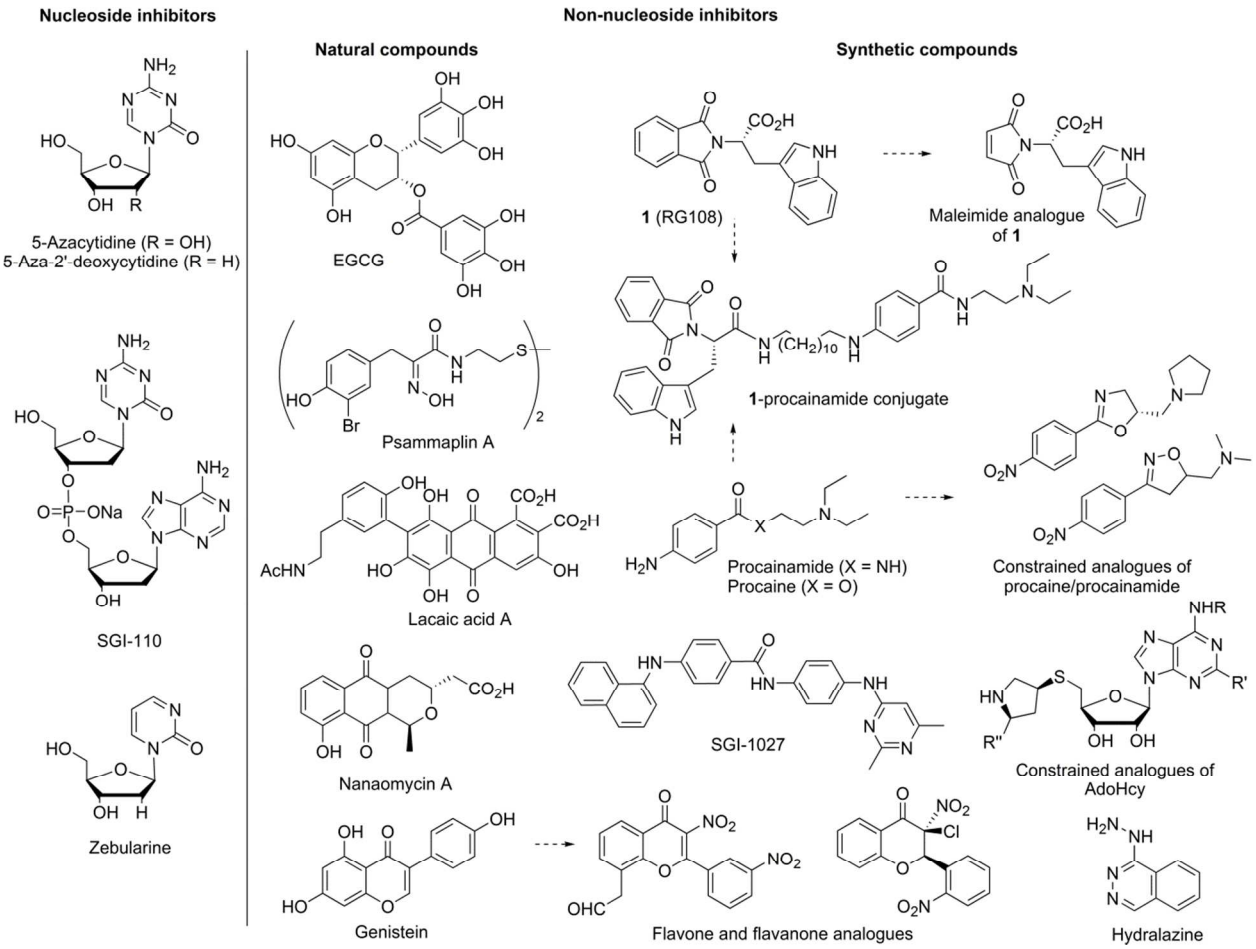

Figure 2. *N*-Phthaloyl-L-tryptophan **1** and its designed analogues

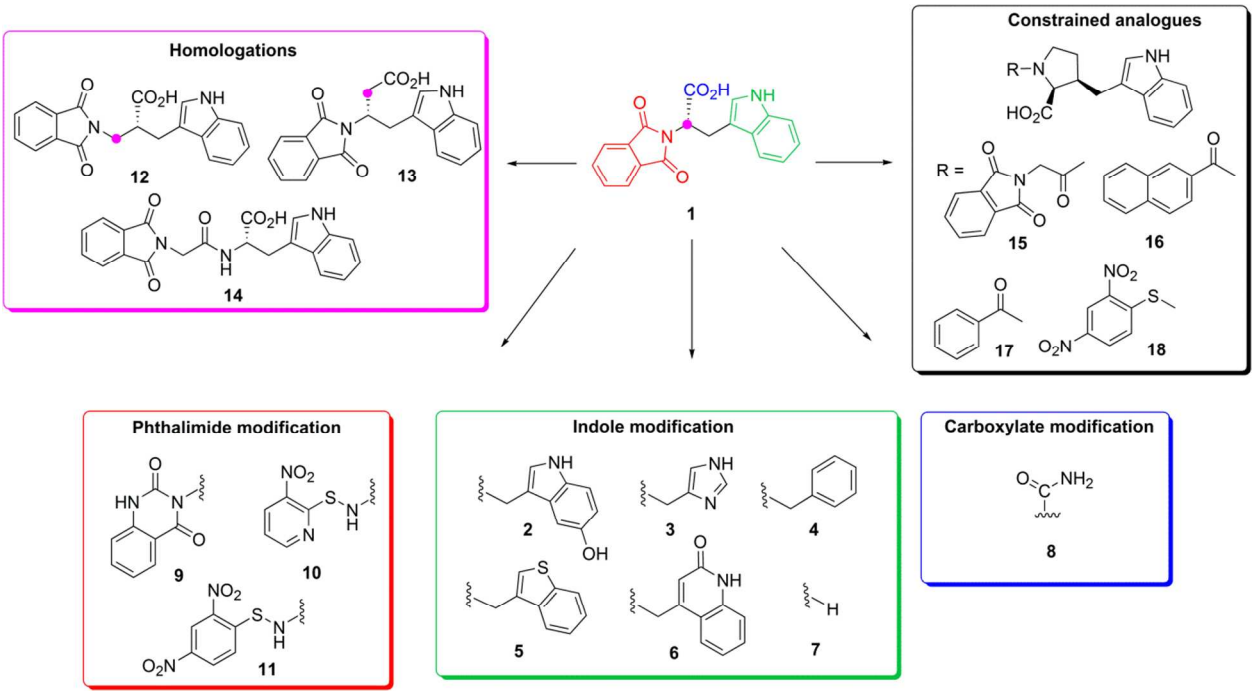

Figure 3. The *in vitro* DNMT1 activity is expressed as the percentage of the value in the absence of inhibitors, taken as 100%. All compounds were tested at 500 μM in the presence of 5% DMSO. Error bars indicate standard deviations of each measurement.

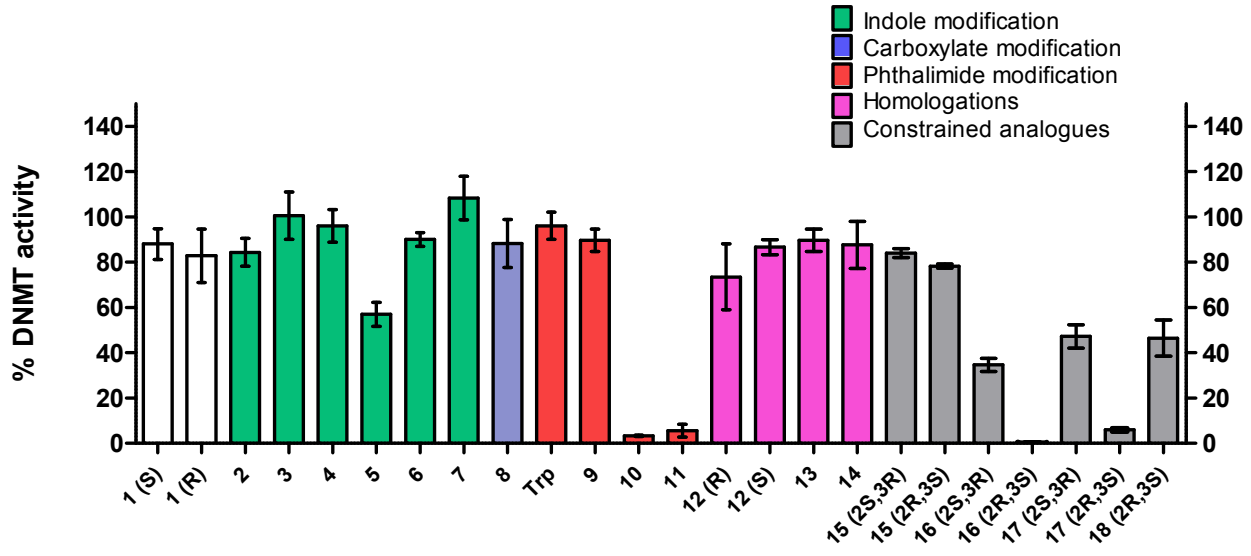

Figure 4. 1D NMR spectra showing the competition between AdoHcy and **1** in binding to the *C*-terminal catalytic domain of the murine Dnmt3A. (a) 1D ^{1}H NMR spectrum of AdoHcy. Resonances at 8.36 and 8.26 ppm correspond to the adenine protons of AdoHcy. F label indicates the signal of formic acid contaminant. (b, c) WaterLOGSY spectrum of 0.45 mM AdoHcy in the absence (b) and in the presence (c) of 8 μM Dnmt3A. Im labels correspond to ^{1}H signals of imidazole contaminant coming from enzyme solution. (d) WaterLOGSY spectrum of 0.45 mM AdoHcy in the presence of 8 μM Dnmt3A and 0.85 mM **1**. (e) Corresponding 1D reference spectrum of AdoHcy in the presence of Dnmt3A and **1**. Signals around 7.7 ppm correspond to phthalimide protons of **1** and signals in the 7–7.6 region correspond to the indole protons of **1**. The formic acid and imidazole contaminants display positive NOEs with bulk water (b–d), indicating the absence of binding to Dnmt3A.

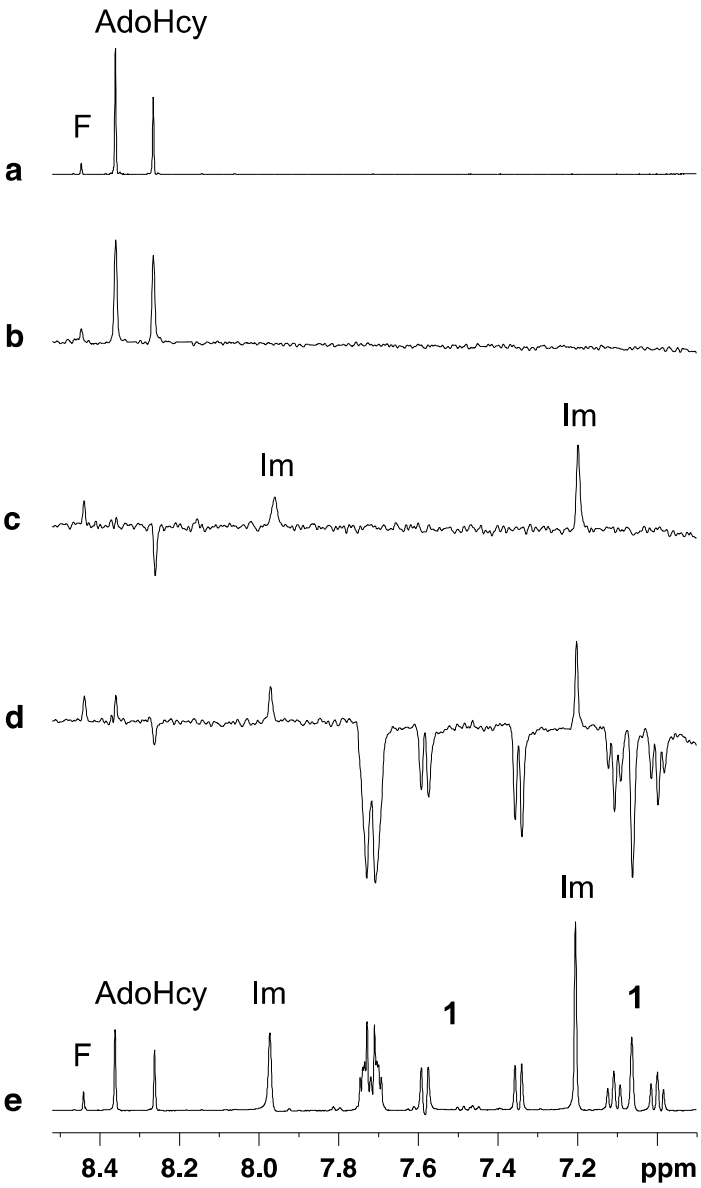
AdoHcy
F
a
b
Im
Im
c
d
Im
AdoHcy
Im
1
1
F
e
8.4
8.2
8.0
7.8
7.6
7.4
7.2
ppm

Figure 5. IFD of **1** (**A**) and superimposed to compound 5 (in green) (**C**) of Suzuki *et al.*[38] by SYBYL-X 1.3 in the three-dimensional structure of the catalytic murine Dnmt1 (residues 732-1600) containing AdoHcy (from PDB 4DA4). 2D ligand interaction diagram of **1** with the essential amino acid residues at the binding site (**B**). The purple circles show the amino acids which participate in hydrogen bonding, electrostatic or polar interactions and the green circles show the amino acids which participate in the Van der Waals interactions. Hydrogen bonds between **1** and amino acids are shown in dashed blue lines. (**D**) IFD of compound **16** (2*R*, 3*S*) shown in two orientations. (**E**) 2D ligand interaction diagram of **16** with the essential amino acid residues at the binding site.

Inhibitors are shown in stick representation in grey, ligands AdoHcy and cytidine are represented in green. The amino acids close (< 5 Å) are shown. Heteroatoms are colored: oxygen in red, nitrogen in blue, sulfur in yellow. H-bonds are shown. The hydrophobicity of the protein surface is indicated.

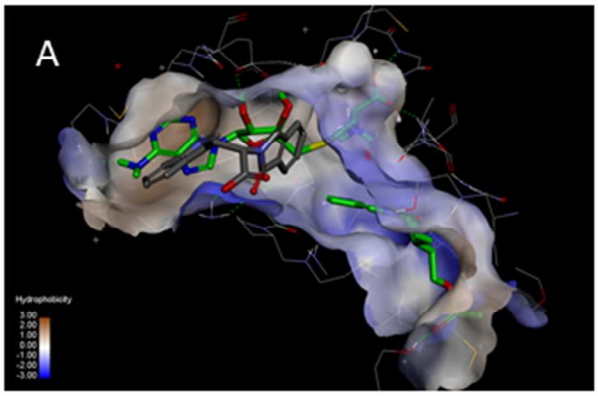
A
Hydrophobicity
3.00
2.00
1.00
0.00
-1.00
-2.00
-3.00

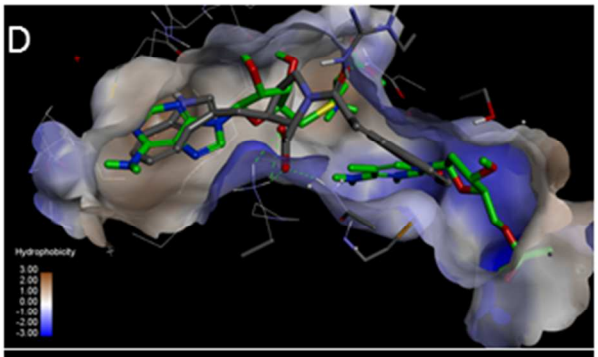
D
Hydrophobicity
3.00
2.00
1.00
0.00
-1.00
-2.00
-3.00

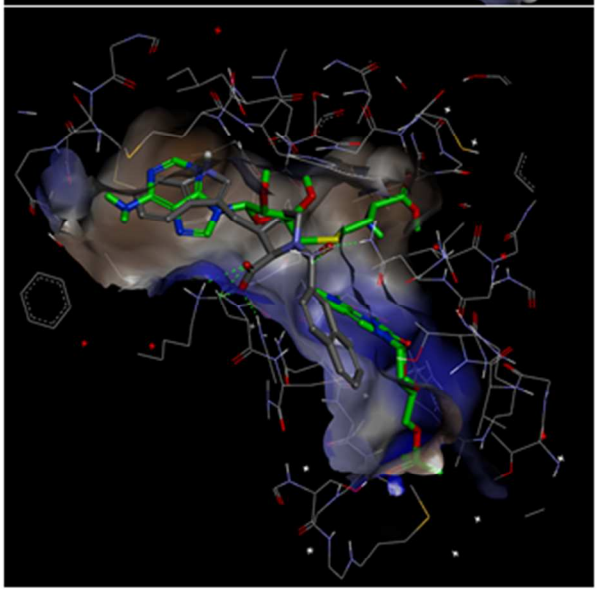

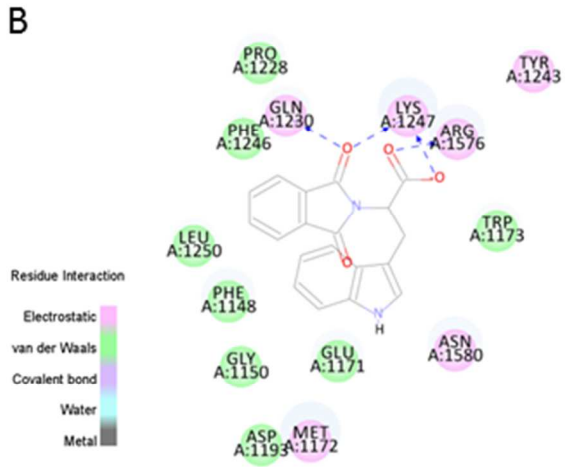
B
PRO A:1228
TYR A:1243
GLN A:1230
LYS A:1247
PHE A:1246
ARG A:1576
TRP A:1173
LEU A:1250
PHE A:1148
GLY A:1150
GLU A:1171
ASN A:1580
ASP A:1193
MET A:1172
Residue Interaction
Electrostatic
van der Waals
Covalent bond
Water
Metal

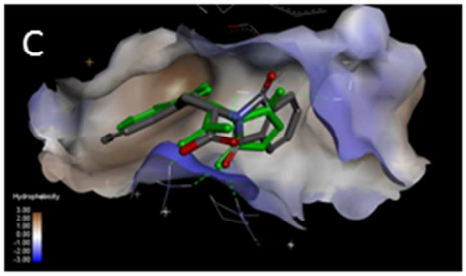
C
Hydrophobicity

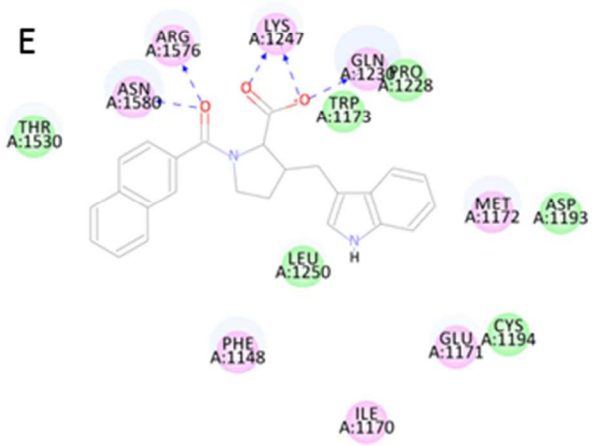
E
ARG A:1576
LYS A:1247
GLN A:1230
PRO A:1228
ASN A:1580
TRP A:1173
THR A:1530
MET A:1172
ASP A:1193
LEU A:1250
PHE A:1148
GLU A:1171
CYS A:1194
ILE A:1170

SCHEMES

Scheme 1. Synthesis of compounds **2-6**, **8**, **13** [a]

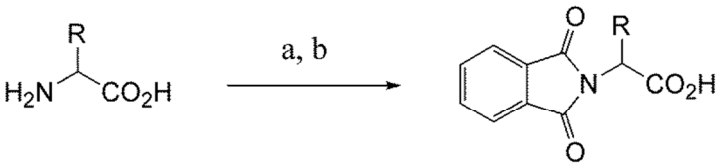

2-6, **8**, **13**

[a] Reagents and conditions: (a) Na_2CO_3, 5 eq, $MeCN/H_2O$; (b) MSB (11-35%)

Scheme 2. Synthesis of quinazolinedione derivative **9** and arylsulphenyl derivatives **10** and **11** [a]

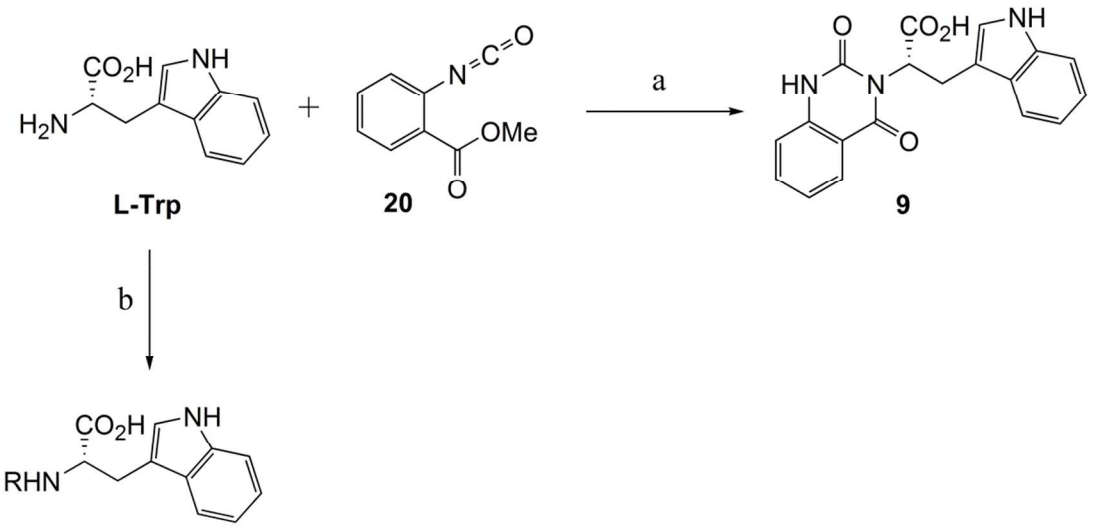

10 R = 2-nitropyridinylsulfenyl
11 R = 2,4-dinitrophenylsulfenyl

[a] Reagents and conditions: (a) NaOH 1M, dioxane/H_2O, 50°C (10%); (b) nitropyridinylsulfenyl chloride, NaOH 2M, dioxane (50%) (**10**) or 2,4-dinitrophenylsulfenyl chloride, NaOH 2M, dioxane (70%) (**11**)

Scheme 3. Synthesis of β2-analogues **12** [a]

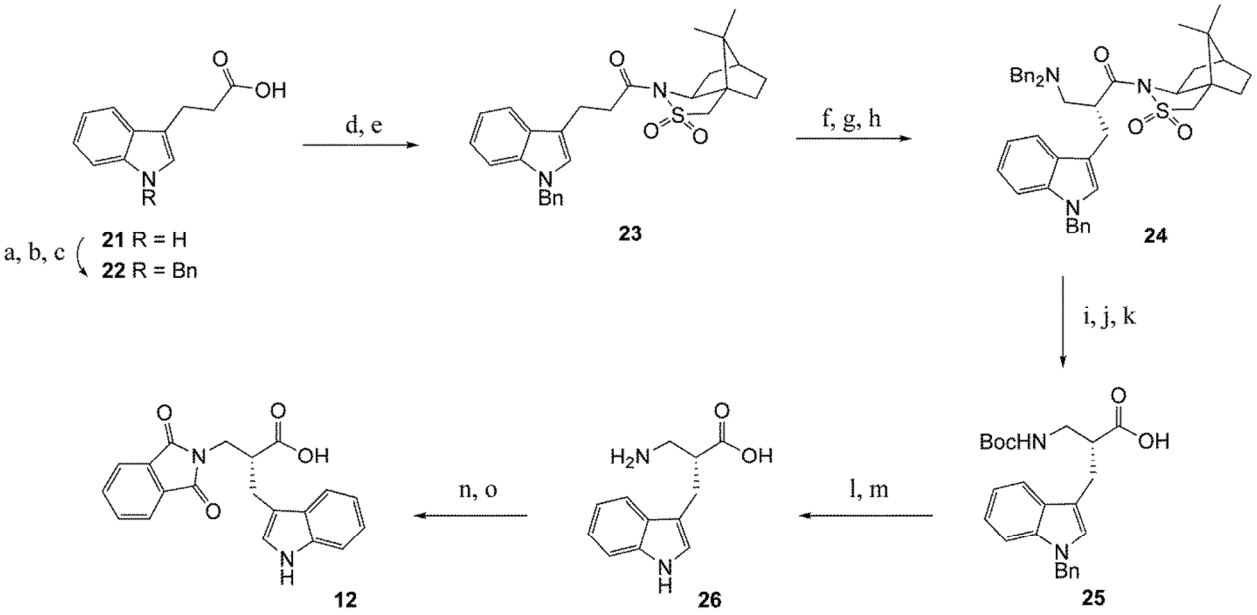

[a] Reagents and conditions: (a) NaH eq., DMF, 0°C; (b) BnBr; (c) LiOH (75%); (d) *i*-BuOCOCl, NMM, DME, -15°C; (e) Sultam sodium salt (70%); (f) TMSOTf, NEt_3 ; (g) $CH_2{=}NBn_2CF_3CO_2$; (h) TBAF (88%); (i) H_2, $Pd(OH)_2$, THF/MeOH; (j) LiOH, MeCN/H_2O; (k) Boc_2O, LiOH, H_2O/dioxane (65%); (l) Na/NH_3, THF, -50°C (48%); (m) TFA (quantitative); (n) Na_2CO_3, 5 eq, MeCN/H_2O, room temperature ; (o) MSB (11%).

Scheme 4. Synthesis of the dipeptide **14** [a]

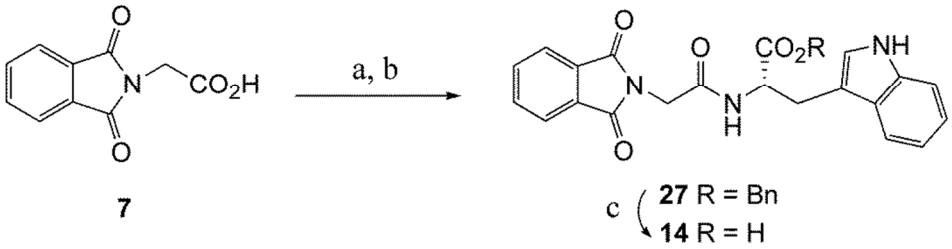

[a] Reagents and conditions: (a) NMM 2eq, isobutyl chloroformate 1eq, THF, -15°C ; (b) L-Tryptophan benzyl ester, THF, -15°C to room temperature (78%); (c) H_2, Pd/C, THF, (60%).

Scheme 5. Synthesis of prolino-analogues **15-18** [a]

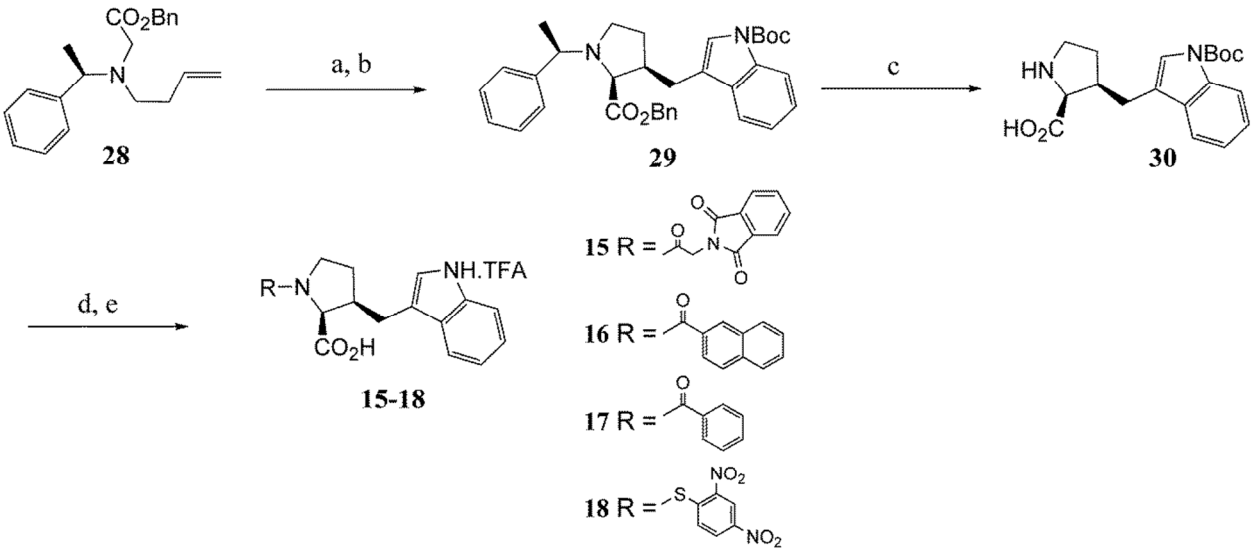

[a] Reagents and conditions: (a) 2eq. LDA, 2eq. $ZnBr_2$; (b) *N*-Boc-3-iodo-indole, $Pd(OAc)_2$, (*t*-Bu_3PH)-BF_4, -78°C (60%); (c) H_2 (5 bar) Pd/C MeOH (79%); (d) *N*-phthaloylglycine, HATU, DIPEA, DMF (20%) (**15**) or naphthoyl chloride, NEt_3, CH_2Cl_2 (63%) (**16**) or benzoyl chloride, NEt_3, CH_2Cl_2 (67%) (**17**) or 2,4-dinitrophenylsulfenyl chloride, NaOH 2M, dioxane (55%) (**18**); (e) TFA (quantitative).

TABLES.

Table 1. Inhibition of human DNMT1 by the most active compounds. The cytotoxicity on DU145 cell lines is reported as TC_{50} (μM).

Cpds	DNMT1 IC_{50} (μM) [a]	DU145 TC_{50} (μM) [b]
1	390 ± 50	660 ± 50
5	230 ± 50	ND
10	20 ± 6	211 ± 80
11	40 ± 8	103 ± 30
16 (2*S*,3*R*)	128 ± 28	280 ± 30
16 (2*R*,3*S*)	50 ± 14	130 ± 30
17 (2*S*,3*R*)	98 ± 3	230 ± 50
17 (2*R*,3*S*)	73 ± 14	232 ± 50
18 (2*R*,3*S*)	80 ± 20	250 ± 50

[a] mean value (± SE) of the concentration at which 50% of inhibition of the enzyme activity is observed. [b] mean value (± SE) of the concentration at which 50% of inhibition of cellular proliferation is observed. N.D.= not determined

Table of Contents / Abstract Graphic

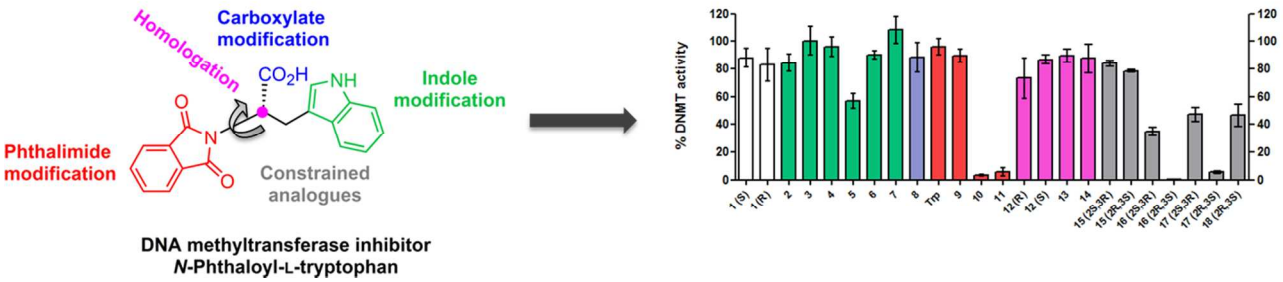

DNA methyltransferase inhibitor
N-Phthaloyl-L-tryptophan